

ANNIHILATION EMISSION FROM THE GALACTIC BLACK HOLE

K. S. Cheng¹, D. O. Chernyshov^{1,2}, and V. A. Dogiel^{1,3}

ABSTRACT

Both diffuse high energy gamma-rays and an extended electron-positron annihilation line emission have been observed in the Galactic Center (GC) region. Although X-ray observations indicate that the galactic black hole Sgr A* is inactive now, we suggest that Sgr A* can become active when a captured star is tidally disrupted and matter is accreted into the black hole. As a consequence the galactic black hole could be a powerful source of relativistic protons. We are able to explain the current observed diffuse gamma-rays and the very detailed 511 keV annihilation line of secondary positrons by $p-p$ collisions of such protons, with appropriate injection times and energy. Relativistic protons could have been injected into the ambient material if the black hole captured a $50M_{\odot}$ star at several tens million years ago. An alternative possibility is that the black hole continues to capture stars with $\sim 1M_{\odot}$ every hundred thousand years. Secondary positrons produced by $p-p$ collisions at energies $\gtrsim 30$ MeV are cooled down to thermal energies by Coulomb collisions, and annihilate in the warm neutral and ionized phases of the interstellar medium with temperatures about several eV, because the annihilation cross-section reaches its maximum at these temperatures. It takes about ten million years for the positrons to cool down to thermal temperatures so they can diffuse into a very large extended region around the Galactic center. A much more recent star capture may be also able to account for recent TeV observations within 10 pc of the galactic center as well as for the unidentified GeV gamma-ray sources found by EGRET at GC. The spectral difference between the GeV flux and the TeV flux could be explained naturally in this model as well.

Subject headings: comic rays : general - Galaxy : center - Galaxies : gamma-rays - black hole - radiation mechanisms : nonthermal

¹ Department of Physics, University of Hong Kong, Pokfulam Road, Hong Kong, China;

² Moscow Institute of Physics and Technology, Institutskii lane, 141700 Moscow Region, Dolgoprudnii, Russia;

³I.E.Tamm Theoretical Physics Division of P.N.Lebedev Institute, Leninskii pr, 53, 119991 Moscow, Russia.

1. Introduction

The annihilation of cosmic ray positrons produced as a result of cosmic ray proton collisions with the ambient plasma was discussed in a number of papers (see, e.g., Ginzburg and Syrovatskii, 1964; Hayakawa et al. 1964; Stecker 1969; Bussard et al. 1979, etc.). A typical cosmic ray positron resulting from secondary π -meson decay may undergo one of three fates: 1) escape from the Galaxy, 2) annihilate with an electron while at relativistic energy (*in-flight annihilation*), or 3) lose almost all its energy before annihilation. One can consider that annihilation may occur either between free electrons and positrons (*free annihilation*), or through the formation of the intermediate bound state of positronium. Positronium can form in either a singlet state, which annihilate into two 511 keV photons, or in a triplet state which decays by three photon annihilation producing a continuum emission below 511 keV (see Ore and Powell 1949).

The cross-section for positron annihilation as a function of energy was given first by Dirac (1930) (see also Heitler 1960).

Radiation from electron-positron annihilation from the central region of our Galaxy was first reported more than 30 years ago (Johnson et al. 1972). In 1978 it was reported that there is a flux of the positron annihilation line (see Leventhal et al. 1978) which might be produced in a compact source at or near the Galactic center. First estimations of the morphology of this line was obtained by the OSSE telescope on-board the Compton observatory (see, e.g., Cheng et al. 1997). With the launch of the INTEGRAL telescope high resolution spectroscopy with reasonable angular resolutions became available. These measurements showed a flux of the annihilation emission from the central bulge. The bulge annihilation emission is highly symmetric with an extension of 8° . The INTEGRAL team measured a 511 keV line, of width 2.2 keV, with a flux $(1.01 \pm 0.02) \times 10^{-3}$ ph cm $^{-2}$ s $^{-1}$ and an ortho-positronium annihilation continuum flux equal TO $(4.3 \pm 0.3) \times 10^{-3}$ ph cm $^{-2}$ s $^{-1}$ (see Teegarden et al. 2005; Knoedlseder et al. 2005; Churazov et al. 2005; Jean et al. 2005).

From the ratio between line and continuum intensities near and below 511 keV it was concluded that positrons annihilate via positronium formation. The fraction of positronium was estimated to be in the region of 92-97% (Weidenspointner et al. 2006; Jean et al. 2005). From the observed width of the annihilation line it was concluded (see Churazov et al. 2005; Jean et al. 2005) that the annihilation of thermal positrons takes place in a relatively warm (several eV) and lowly ionized (~ 0.1) interstellar medium.

The origin of such positrons is still poorly understood. A large variety of positron sources have been proposed. Among them novae and supernovae stars (Chan and Lingenfelter 1993; Dermer and Murphy, 2001). However, as follows from Weidenspointner et al. (2005) the

annihilation of positrons appears to be even more concentrated in the bulge than are old stellar populations such as Type Ia supernovae, novae, or low-mass X-ray binaries. New, speculative, physics such as positron production from hypernovae stars (Casse et al. 2004), light dark matter (see Boehm et al. 2004) etc. has begun to be discussed as a possible solution. A supermassive black hole of $2.45 \times 10^6 M_\odot$ is another candidate as a source of positrons. Thus, Zheleznyakov and Belyanin (1994) concluded that the annihilation emission is consistent with a model in which electron-positron pairs, created in the vicinity of a black hole, are trapped in the magnetosphere supported by an accretion disk.

Secondary positrons generated as a result of cosmic ray collisions with the ambient plasma is another alternative model. Melia et al. (1998); Fatuzzo et al. (2001) and Fatuzzo and Melia (2003) suggested a supernova coinciding with the central radio source Sgr A East as an emitter of protons which can produce gamma-rays as well as high energy secondary positrons. However, they showed from simplified equations that Sgr A East could not be the source of annihilation radiation from the Galactic center because, based on their estimates, the thermalization time was too long. Besides, the annihilation emission appears to be diffuse. So far, there is no evidence for emission from point-like sources (Knoedlseder et al. 2005; Bouchet et al. 2005). On the other hand, the EGRET telescope found a flux of gamma-rays from the Galactic center at energies > 500 MeV (Mayer-Hasselwander et al. 1998) which was seen as a strong excess of gamma-rays peaking in an error circle of 0.2° radius surrounded by a strong emission maximum within $\sim 5 - 8^\circ$ degrees from the Galactic center.

In our model we assume the black hole is a source of high energy protons generated by star accretion. They produce secondary gamma-rays and relativistic positrons as a result of $p - p$ collisions. The secondary positrons requires over 10 million years to cool down before annihilation. Hence they are able to propagate far away from the central source during their lifetime and to fill a sphere with the radius about several hundred pc. Therefore the annihilation emission can be seen as diffuse if these protons were ejected a relatively long time ago. From kinetic equations we shall show that processes of Coulomb collisions are effective enough to cool down these relativistic positrons and to thermalize them before their annihilation, which can explain the origin of the annihilation emission from the Galactic center.

2. Energy Release Supplied by a Black Hole

We will first summarize how much energy must be released from the Galactic black hole in order to explain the observed X-rays, diffuse gamma-rays, the annihilation emission and

TeV emission.

2.1. X-rays

The ASCA telescope found hard X-ray emission from in the energy range 2-10 keV the central part of the Galactic plane (Koyama et al. 1996). The total thermal energy of the hot plasma component inside a 1° region around the Galactic center was estimated to be $10^{52} - 10^{53}$ erg. A large energy generation rate in the Galactic Center is required $\sim 10^{41} - 10^{42}$ erg s^{-1} and a supernova origin of this emission seems to be implausible.

Recently, *Chandra* observations showed intense X-ray emission at energy $E_x \sim 8$ keV from the inner 20 pc of the Galaxy, with a luminosity $L_x \sim 10^{38}$ erg s^{-1} . We know of no class of object which can provide this luminosity there. Therefore this emission was interpreted as thermal emission of an optically thin plasma with a temperature of 8 keV. However, for the gravitational potential near the Galactic center (see Breitschwerdt et al. 1993) the escape velocity is about 900 km s^{-1} . The sound speed of an 8 keV plasma is 1500 km s^{-1} and the required power necessary to compensate the plasma outflow is $\sim 10^{40}$ erg s^{-1} . This is equivalent to the entire of supernova kinetic energy output occurring every 3,000 years, and is unreasonably high (Muno et al. 2004).

2.2. Gamma-rays.

The EGRET telescope (see Mayer-Hasselwander et al. (1998)) found a gamma-ray flux toward the Galactic Center of the order of 2×10^{37} erg s^{-1} for energies $E_\gamma > 500$ MeV in an error circle of 0.2° radius. The photon spectrum from the center (ph $cm^{-2}s^{-1}$) can be represented as

$$F(E_\gamma) \simeq 2.2 \times 10^{-10} \left(\frac{E_\gamma}{1900 \text{ MeV}} \right)^{-1.3} \quad (1)$$

for $E_\gamma < 1900$ MeV

and

$$F(E_\gamma) \simeq 2.2 \times 10^{-10} \left(\frac{E_\gamma}{1900 \text{ MeV}} \right)^{-3.1} \quad (2)$$

for $E_\gamma > 1900$ MeV

The bulk of the emission is most compatible with it originating in a volume with a radius 85 pc though, in view of uncertainties, the source excess is marginally compatible with emission from a single compact object. If we assume that the central gamma-ray source is due to injection of relativistic protons we can estimate their energy. The flux of gamma-rays from the central source is about $F_\gamma \simeq 2 \cdot 10^{37} \text{ erg s}^{-1}$. The lifetime of relativistic protons in the interstellar medium with a density $n \simeq 1 - 10 \text{ cm}^{-3}$ is about $\tau_p \simeq 10^{14} - 10^{15} \text{ s}$, which gives a total energy in relativistic protons $W_p \simeq F_\gamma \cdot \tau_p \sim 10^{52} \text{ erg}$. This is more than can be supplied by the most powerful known galactic source of energy, such as a supernova, whose total energy release is about 10^{51} erg .

2.3. Annihilation line emission

On the basis of the reported flux of annihilation line emission (see Teegarden et al. 2005; Knoedlseder et al. 2005; Churazov et al. 2005; Jean et al. 2005), the annihilation rate of positrons is roughly $\sim 10^{43} \text{ s}^{-1}$. Assuming that each interaction of a relativistic proton with an average energy about 1 GeV produces one secondary positron, we find that the injected energy rate of protons is $\dot{W}_p \sim 10^{40} \text{ erg s}^{-1}$. The total amount of injected proton energy must be of the order (or smaller than) $W_p \sim \dot{W}_p \tau_c \sim 10^{54} \text{ erg}$, where $\tau_c \sim 10^{14} \text{ s}$ is the cooling time of relativistic positrons in the interstellar medium with a gas density $n \sim 1 \text{ cm}^{-3}$. Such a huge amount of energy is the most important constraint of the model. In section 2.5, we will discuss some possible energy injection mechanisms.

2.4. TeV gamma-rays

TeV gamma-ray emission from the Galactic black hole Sgr A* was first reported by the Whipple group (Buckley et al. 1997). More recently it has been confirmed by three independent groups, Whipple (Kosack et al. 2004), CANGAROO (Tsuchiya et al. 2004), and HESS (Aharonian et al. 2004) at a luminosity $> 10^{35} \text{ ergs s}^{-1}$. If these TeV gamma-rays are produced via p - p collisions, the possible input proton energy could be 10^{50-52} erg depending on the proton injection spectrum and the diffusion coefficient (Aharonian and Neronov 2005a).

Thus, observational data indicate a huge energy release at the Galactic center with an energy of the order $> 10^{52} \text{ erg}$, which cannot be supplied by known Galactic sources, and a significant part of this energy is enclosed in the form of relativistic protons. One can assume that such energy can be released when a star is disrupted near a black hole.

2.5. Theoretical estimates.

The rate at which a massive black hole in a dense star cluster tidally disrupts and swallows stars has been studied extensively (e.g. Hills 1975; Bahcall and Wolf 1976; Lightman and Shapiro 1977). Basically when a star trajectory happens to be sufficiently close to a massive black hole, the star would be captured and eventually disrupted by tidal forces. After a dynamical time-scale (orbital time-scale), the debris of a tidally disrupted star will form a transient accretion disk around the massive black hole, with a radius typically comparable to the tidal capture radius (Rees 1988). Rees has also argued that most of the debris material will be swallowed by a black hole with a mass $\sim 10^6 M_\odot$ on a time scale of ~ 1 yr for a thick hot ring, or $\sim 10^2$ yrs for a thin cool disk, respectively. The capture rate is essentially a problem of loss-cone diffusion-diffusion in angular momentum rather than energy. By assuming a Salpeter mass function for the stars, Syer and Ulmer (1999) have estimated the capture rate in our Galaxy as $\sim 4.8 \times 10^{-5} \text{yr}^{-1}$ for main sequence stars and $\sim 8.5 \times 10^{-6} \text{yr}^{-1}$ for red giant stars, respectively. However, the actual capture rate depends sensitively on the assumed mass function of stars, the stellar evolution model used, the radius and mass of the captured star, the black hole mass and the internal dispersion velocity of stars (v_s) around the black hole. For example, Cheng and Lu (2001) obtained a longer capture time $\sim 10^6$ years, by taking $v_s = 10^2 \text{km/s}$ and $M_{bh} = 2.45 \times 10^6 M_\odot$. Therefore the capture time for a main sequence star with mass $\sim 1 M_\odot$ could range from several ten thousand years to several hundred thousand years. The capture time for the more massive stars is expected to be even longer. For $t > t_{peak}$, the accretion rate evolves as, Rees (1988); Phinney (1989)

$$\dot{M} \sim \frac{1}{3} \frac{M_*}{t_{min}} \left(\frac{t}{t_{min}} \right)^{-5/3} \quad (3)$$

where M_* and R_* are the mass and the radius of the captured star, respectively and $t_{peak} \sim 1.59 t_{min}$, where

$$t_{min} \approx 0.2 \left(\frac{M_\odot}{M_*} \right) \left(\frac{R_*}{R_\odot} \right)^{3/2} \left(\frac{M_{bh}}{10^6 M_\odot} \right)^{1/2} \text{yr} \quad (4)$$

is the characteristic time for the debris to return to the pericenter (Lu et al. 2005). The recent *Chandra* observations of three large amplitude, high-luminosity soft X-ray flares in AGNs provide strong evidence for the tidal capture events, and the decrease of X-ray luminosity indeed follows closely the above theoretical predictions (e.g. Halpern, Gezari and Komossa 2004).

Sirota et al. (2005) analyzed the tidal disruption of stars near a black hole, a process which is a possible mechanism for the activity of galactic nuclei. They concluded that the total power released during the destructions of a star is on average $4 \cdot 10^{43} \text{erg s}^{-1}$. However, the duration of the energy emission due to the absorption of a star (~ 200 years) is much

shorter than the mean time between two absorption events. Therefore most of the time galactic nuclei are in a low active state. Furthermore, the maximum energy release must be much higher than the mean estimate. For example, the highest luminosity observed in PG 0052+251 (see Table 1 in Sirota et al. 2005) is 5×10^{44} erg s $^{-1}$, which gives a total energy release during 200 years of about 3×10^{54} erg.

It is very important to know how much of the accretion power will be converted into the out-flow of relativistic protons. Processes of particle acceleration near black holes are not well known though several models of particle acceleration in accretion disks and jets of black holes have been developed (see, e.g., Kardashev 2001; Heinz and Sunyaev 2002; Le Truong and Becker 2004; Aharonian and Neronov 2005b). For our aims we estimate roughly from Eq.(3) the energy of disruption which can be transferred to protons. In the case of star capture, it is very natural to assume that the resulting jet contains mainly protons simply because of the dominance of hydrogen in stars. We do not know how the jet is formed but if we take the analogy of Active Galactic Nuclei (AGN), then we can argue that the observed Doppler factor of AGN is of order 10, and we just assume that the jet coming out from our galactic black hole is mildly relativistic and its main composition is protons.

Falcke and Biermann (1999) have argued that the conversion efficiency (η_p) from accretion power ($\dot{M}c^2$) into the the energy of jet motion ranges from 10^{-1} to 10^{-3} . Integrating the Eq.(3) and using typical values of the parameters, the energy carried away by relativistic protons is estimated as

$$\Delta E_p \sim 6 \times 10^{52} (\eta_p / 10^{-1}) (M_*/M_\odot) \text{erg}. \quad (5)$$

In addition to the accretion power, Cheng and Lu (2001) have argued that if the transient accretion disk can generate a sufficiently strong magnetic field, due to the instability of the disk, this strong magnetic field can initiate the Blandford-Znajek process (Blandford and Znajek 1977) to extract rotation energy from the black hole. They estimate that the maximum energy that can be extracted from a black hole is given by

$$\Delta E_{max} \sim 3 \times 10^{52} A^2 f(A) M_6^2 \text{erg}. \quad (6)$$

where A is the dimensionless angular momentum of the black hole, $f(A)$ is a constant for given A and M_6 is the black hole mass in units of $10^6 M_\odot$. If the black hole is rotating in maximum angular velocity, $A = 1$, then $f(A)=1.14$.

The maximum energy in relativistic protons can be estimated from Eq.(5) or (6). If a star with the mass about $50 M_\odot$ is captured by a black hole, it gives an energy in relativistic protons as high as $\sim 10^{54}$ erg.

Thus, we conclude that when eventually a massive star is captured, a huge amount of energy can be released in the form of relativistic protons during a very short time. Below we assume that such primary protons interact with the medium gas in the region, its intensity derived from the gamma-ray data, and produce there secondary gamma-rays and positrons.

In the summary of these two sections we present the conditions which our model of annihilation emission by the black hole should satisfy:

1. The rate of production of thermal positrons at present should be $\sim 10^{43} \text{ s}^{-1}$;
2. If positrons are produced via $p - p$ collisions the total energy of relativistic protons must not exceed $10^{53} - 10^{54} \text{ erg}$;
3. The eruption time of protons is much smaller than any other characteristic time of the problem. Therefore the production function of protons can be described as a delta function in time;
4. Though positrons are emitted by the black hole - a point-like source- their spatial distribution when they cool down to thermal energies should extend over a region with an angular radius $5^\circ - 8^\circ$ around the Galactic Center;
5. If the gamma-ray emission near the Galactic center and the annihilation emission have a common origin the flux of gamma-rays with energies $E_\gamma > 500 \text{ MeV}$ should be about $F_\gamma \sim 2 \cdot 10^{37} \text{ erg s}^{-1}$.

3. Proton Spectrum

We take the source function of protons as

$$Q(r, E_p, t) = A(E_p)\delta(\mathbf{r})\delta(t) \quad (7)$$

Particles can be accelerated near the hole by a shock wave appearing in the accreting matter. According to typical shock acceleration models the momentum spectrum of accelerated particles is a power-law, with a spectral index γ_0 between 2-3. If we transform the

momentum spectrum to an energy spectrum, then it has the form

$$A(E_p) = A'_0 \frac{E_p + M_p c^2}{(E_p^2 + 2M_p c^2 E_p)^{(\gamma_0+1)/2}} \quad (8)$$

In fitting the observed diffuse gamma-ray spectrum we should be able to provide some constraints on γ_0 . However, the error bars of the observed data are quite large (cf. Fig. 3), and the possible range of γ_0 is around 2.6-3.1. In fact the best fit gamma-ray spectral index is 3.1 for photon energies larger than 2 GeV (cf. Eq.2). However, the exact value of γ_0 affects neither the gamma-ray luminosity nor the annihilation flux significantly, because most of the energy comes from protons with energies of several GeV. Below we take $\gamma_0 \sim 2.6$ as reference and the constant A'_0 will be found from the gamma-ray data.

The spatial distribution of the protons can easily be derived from the well-known equation of cosmic ray propagation (see Berezhinskii et al. 1990),

$$\frac{\partial n_p}{\partial t} - \nabla(D_x \nabla n_p) + \frac{\partial}{\partial t} \left(\frac{dE}{dt} n_p \right) + \frac{n_p}{\tau_p} = Q(\mathbf{r}, E_p, t) \quad (9)$$

Here dE/dt is the term describing particle energy losses and τ_p is the characteristic time of catastrophic losses.

In the relativistic energy range the lifetime of protons is determined by $p-p$ collisions, and equals $\tau_p \simeq 10^{15}$ s for a gas density $n = 1 \text{ cm}^{-3}$. The rate of continuous energy loss is negligible in this energy range ($dE/dt \simeq 0$). The solution of Eq. (9) in this case is similar to the solution of the equation of thermal conductivity

$$n_p(r, E_p, t) = A \exp[-t/\tau_p] \frac{\exp\left[-\frac{r^2}{4D_x t}\right]}{(4\pi D_x t)^{3/2}} \quad (10)$$

and describes an almost uniform proton distribution within the sphere of the radius $r \lesssim \sqrt{D_x t}$.

In the non-relativistic energy range the injection spectrum is transformed by ionization losses which for a medium density $n = 1 \text{ cm}^{-3}$ are significant at relatively low proton energies. The rate of ionization losses is (Hayakawa 1964; Ginzburg 1989)

$$\frac{dE}{dt} = -\frac{2\pi e^4 n}{mc\beta(E)} \ln\left(\frac{m^2 c^2 W_{max}}{4\pi e^2 \hbar^2 n}\right) \simeq -\frac{a}{\sqrt{E}} \quad (11)$$

where W_{max} is the highest energy transmitted to an ambient electron, and $\beta(E) = v/c$. The characteristic time of ionization (Coulomb) losses is $\tau_c \sim E/(dE/dt)$. Variations of ionization loss times for electrons (dashed-dotted line) and protons (solid line) are shown in Fig.1.

The equation for the total number of particles $N(E, t) = 4\pi \int_0^\infty n_p(E, r, t) r^2 dr$ can be obtained by integration of Eq.(9) over the volume occupied by the particles when $dE/dt \neq 0$ and is described by Eq.(11),

$$N_p(E_p, t) = \frac{2}{3} \frac{A_0 \sqrt{E_p}}{\left(\frac{3at}{2} + E_p^{3/2}\right)^{(\gamma_0+2)/3}} \frac{\left[\left(\frac{3at}{2} + E_p^{3/2}\right)^{2/3} + M_p c^2\right]}{\left[\left(\frac{3at}{2} + E_p^{3/2}\right)^{2/3} + 2M_p c^2\right]^{(\gamma_0+1)/2}} \exp\left(-\frac{t}{\tau_p}\right) \quad (12)$$

The total spectrum of protons for an arbitrary constant A_0 is shown in Fig.2. We see that at the initial stage the spectrum is evolved under the influence of ionization loss but after the time $t > \tau_p \sim 10^{15}$ s the $p - p$ nuclear reactions become also essential.

4. The Gas Components and Particle Propagation in the Bulge Region

The gas content in the Galactic center is not well known though one can find its characteristics in Jean et al. (2005). For the interstellar medium several components of the gas were suggested from radio and X-ray data (see the review of Ferrière 2001). They are: a cold neutral component ($n = 10 \text{ cm}^{-3}$, $T = 80 \text{ K}$), a warm neutral component ($n = 0.3 \text{ cm}^{-3}$, $T = 8000 \text{ K}$), a warm ionized component ($n = 0.17 \text{ cm}^{-3}$, $T = 8000 \text{ K}$) and a hot component ($n = 3 \cdot 10^{-3} \text{ cm}^{-3}$, $T = 4.5 \cdot 10^5 \text{ K}$). The distribution of these components in the bulge region is strongly nonuniform which complicates matters. The point is that gamma-rays from π^0 can be produced by all components of the gas if high energy protons penetrate there while annihilation photons are produced mainly in the neutral and ionized warm components where the cross-section for annihilation increases by several orders of magnitude as compared with the other components. We do not know whether the propagation of high energy protons is the same in all components of the bulge medium. We also do not know the characteristics of secondary positron propagation: whether they are able to penetrate into dense molecular clouds or what is their diffusion coefficient.

The Bulge (i.e. the region inside a radius $\sim 230 \text{ pc}$ with a height 45 pc) contains $7 \cdot 10^7 M_\odot$ of hydrogen gas. 90% of this mass is trapped in small high density ($\sim 10^4 \text{ cm}^{-3}$) clouds that gives the average gas density in the bulge central region as high as $\sim 700 \text{ cm}^{-3}$ while the remaining $\sim 10\%$ is homogeneously distributed with the average density 10 cm^{-3} . The rest of the gas in the bulge is contained in a region (like an ellipsoid) with a radius 1.75 kpc . The H1 mass is equally distribute between cold and warm neutral gas. The mass of warm and hot ionized gas is about $4 \cdot 10^7 M_\odot$. 90% of this mass is in the warm phase and 10% is in the hot phase.

The diffusion coefficient is unknown in the Bulge region. Berezhinskii et al. (1990) estimated the average value of the diffusion coefficient in the Galactic Disk from analyses of the cosmic ray flux and obtained a value $\sim 10^{27} \text{ cm}^2\text{s}^{-1}$. Jean et al. (2005) presented a very rough estimate of the diffusion coefficient in the Bulge region using the equation derived by Melrose (1980)

$$D \simeq D_B \left(\frac{r_L}{\lambda_{max}} \right)^{1-\delta} \eta^{-1} \quad (13)$$

where $D_B = \frac{1}{3}r_L v$ is the Bohm diffusion coefficient, r_L and v are the particle gyroradius and velocity, respectively, $\lambda_{max} \simeq 100 \text{ pc}$ is the maximum scale of turbulence, $\delta = 5/3$ for a Kolmogorov turbulence spectrum, and $\eta \sim \delta B^2/B^2 \sim 1$ is the pressure ratio of magnetic fluctuations to the main field.

For a magnetic field strength $B \sim 10^{-5}\text{G}$ (see, e.g. LaRosa et al. 2005) the diffusion coefficient of 30 MeV positron is about $10^{27}\text{cm}^2\text{s}^{-1}$. Though the diffusion coefficient decreases with particle energy, just this value determines positron propagation in the Bulge region because the characteristic time $\tau_c \propto E^1$, i.e. positrons spend most of their lifetime with high energy.

The problem of particle penetration into molecular clouds was analyzed by Skilling and Strong (1976); Dogiel and Sharov (1985). In the absence of waves the cosmic ray (CR) flux into clouds should be

$$j(E) \simeq N(E)v \quad (14)$$

where v is the particle velocity. However, CRs of a few MeV excite waves to such a high level that the flux reduces to

$$j(E) \simeq N(E)V_A \quad (15)$$

where the Alfvénic velocity $V_A \ll v$.

Therefore, Alfvén waves generated outside molecular clouds by the flux of cosmic rays are effective at excluding cosmic rays below a few hundred MeV, while particles with higher energies freely penetrate into the clouds. This feature plays a very important role in estimating the amount of injection energy of protons for explaining the observed gamma-rays and the annihilation emission.

As we see from our analysis several characteristic times determines the conditions under which the annihilation flux is formed. These times are:

- The current time from the moment of eruption t :

- The time for nuclear $p - p$ reactions (the lifetime of protons) $\tau_p = nv_p\sigma_{pp}$. For gas densities ranging from 1 to 100 cm^{-3} it ranges from 10^{15}s to 10^{13}s ;
- The cooling time of positrons τ_c (the thermalization time)

$$\tau_c \sim \int_{E_{e+}}^{E_{th}} \frac{dE}{(dE/dt)_c} \quad (16)$$

where $(dE/dt)_c$ is the energy cooling rate, which will be discussed in section 7, E_{e+} and E_{th} are the injected energy and the thermalization energy respectively. For a density n we estimate that $\tau_c \sim 3 \times 10^{14}(n/1 \text{ cm}^{-3})^{-1} \text{ s}$.

In the following sections, we investigate models which are characterized by different ratios between these time scales.

5. Gamma Rays from π^0 -Decay

Pions are produced in $p - p$ collisions whose cross-section is well-known (see, e.g., Stephens and Badhwar 1981; Atoyan 1992; Dermer 1986; Dogiel and Sharov 1990; Strong et al. 2000).

The production function of gamma-rays is

$$q_{\pi^0} = \eta \int_{E_p} N(E_p) v_p n_H d\sigma(E, E_p) \quad (17)$$

where η is a factor depending on the chemical composition of cosmic rays and of the interstellar medium, which for the Galaxy equals 1.6 (Stephens and Badhwar 1981), v_p is the velocity of protons and $d\sigma$ is a differential cross-section for the production of a π^0 of energy E by a cosmic ray proton.

According to Fatuzzo and Melia (2003) the cross-section is

$$\frac{d\sigma(E_p, E_{\pi^0})}{dE_{\pi^0}} = \frac{\sigma_0}{E_{\pi^0}} f_{\pi^0}(x) \quad (18)$$

where $x = E_{\pi^0}/E_p$, $\sigma_0 = 32 \text{ mbarn}$ and $f_{\pi^0}(x) = 0.67(1 - x)^{3.5} + 0.5e^{-18x}$. It is important to note that the above formula is based on the isobar model of Dermer (1986), which is

technically appropriate for a modest range of energies above pion decay threshold. At the highest energies detected by EGRET, the scaling model is more appropriate and this is also given in Dermer (1986).

The emissivity of the photons produced by π^0 -decay (q_γ) can be calculated from (Stephens and Badhwar (1981)):

$$q_\gamma(E_\gamma, t) = 2 \int_{E_{\pi min}}^{\infty} \frac{q_\pi(E_\pi, t)}{\sqrt{E_\pi^2 - m_\pi^2 c^4}} dE_\pi \quad (19)$$

where E_γ and E_π are the energy of the emitted photon and the decaying pion respectively, $E_{\pi min} = E_\gamma + \frac{m_\pi^2 c^4}{E_\gamma}$

The spectrum of expected gamma-ray emission is shown in Fig. 3 together with the EGRET data. From the observational data we concluded that at the present time the constant A_0 is

$$A_0 = 4 \times 10^{55} \text{GeV}^{\gamma_0-1} \quad (20)$$

and the total energy of accelerated protons emitting gamma-rays is

$$W_p = \int_{E_p}^{\infty} E_p N_p(E_p) dE_p \simeq 1.5 \times 10^{53} \text{erg}, \quad (21)$$

for a density $n = 1 \text{ cm}^{-3}$. If we take the average density of the gas in the region of gamma-ray emission $n = 10 \text{ cm}^{-3}$ we obtain $W \simeq 10^{52} \text{ erg}$ for the same production rate of gamma-rays.

Below we determine whether these protons are able to generate enough positrons in order to produce the observed flux of the annihilation line

6. Production Function of Secondary Electrons

Inelastic $p-p$ collisions produce two charged pions for every neutral pion. These charged pions quickly decay into muons, which in turn decay into positrons and electrons, with a resulting emissivity

$$q_e(E_e) = n_H c \frac{m_\pi^2}{m_\pi^2 - m_\mu^2} \int_{E_\mu^{min}}^{E_\mu^{max}} dE_\mu \frac{dP}{dE_e} \int_{E_\pi^{min}}^{E_\pi^{max}} \frac{dE_\pi}{\beta_\pi E_\pi} \int_{E_{th}(E_\pi)} dE_p n_p(E_p) \frac{d\sigma(E_\pi, E_p)}{dE_\pi} \quad (22)$$

The integration limits in the above expressions are determined through kinematic considerations: for example for two-body decay the minimum and maximum energy in units of the

rest mass of the created particles are $\gamma - p$ and $\gamma + p$, where γ is the Lorentz-factor of the source particle and $p = \sqrt{\gamma^2 - 1}$ is its dimensionless momentum. The lepton distribution from a decaying muon is given by the three-body decay probability

$$\frac{dP}{dE_e} = \frac{8pc}{\beta_\mu m_\mu^3 c^6} \int du \frac{u(u^2 \gamma_\mu^2 - m_e^2 c^4)^{1/2}}{(pc - E_e + u)^2} \left(3 - \frac{4\gamma_\mu u}{m_\mu c^2} \right) \left(1 - \frac{E_e(E_e - u)}{p^2 c^2} \right) \quad (23)$$

where $u = (E_e - \beta_\mu pc \cos \theta)$, p is the electron momentum and γ is the Lorentz factor for the designated particle (Fatuzzo and Melia 2003).

The production function of π^\pm secondary electrons is shown in Fig.4. The secondary π^\pm electrons are generated above the threshold energy $E \gtrsim 30$ MeV. Below this energy secondary electrons are produced by Coulomb collisions (knock-on electrons). The cross-section of KO electron production is (see, e.g., Hayakawa 1964; Ginzburg 1989)

$$\sigma_{ko} \simeq 2\pi \left(\frac{e^2}{mc^2} \right)^2 \frac{mc^4}{v^2} \frac{1}{E_e^2} \quad (24)$$

The composition of the production flux is an essential function of particle energy. The electron flux at energies above ~ 30 MeV consists of almost equal parts of positrons and electrons. Below this energy the contribution of positrons is negligible.

From Eqs. (12), (20) and (22) we can estimate the total production rate of relativistic positrons at GC at the present moment directly associated with the current gamma-ray production. It equals

$$\frac{dN_{e^+}}{dt} \simeq 10^{41} \text{s}^{-1}. \quad (25)$$

Below we estimate the number of thermal positrons supplied via $p - p$ collisions after their cooling by Coulomb interactions (ionization losses). The total electron production function for π^\pm and KO electrons is shown in Fig. 4 where we used the results of Daniel and Stephens (1975).

The distribution function of these relativistic positrons is described by Eq.(9). In the relativistic energy range electrons lose energy by synchrotron and inverse Compton emission

$$\frac{dE_e}{dt} = -\frac{32\pi c}{9} \left(\frac{e^2}{mc^2} \right)^2 \frac{c}{mc^2} \left(w_{ph} + 6.2 \cdot 10^{11} \frac{H^2}{8\pi} \right) E^2 = -\beta_1 E^2 \quad (26)$$

The characteristic time of energy loss τ in this case is

$$\xi = \int_E^{E_0} \frac{dE}{\beta_1 E^2} \quad (27)$$

Then for the proton spectrum (10) and the production function (22) the spectrum of secondary electrons can be derived from the general equation (9), see Syrovatskii (1959) and Gratton (1972),

$$N_e(E_e) = \frac{1}{E_e^2} \int_0^t \theta(t_0) dt_0 \int_0^\infty r_0^2 dr_0 \frac{\exp\left[-\frac{r_0^2}{4D_x t_0}\right]}{(4\pi D_x t_0)^{3/2}} \int_0^\eta d\tau \frac{q_e(\eta - \xi)}{(4\pi D_x \xi)^{3/2}} \times \quad (28)$$

$$\times \exp\left[-\frac{(\mathbf{r} - \mathbf{r}_0)^2}{4D_x \tau_0}\right] \delta(t - t_0 - \tau)$$

where

$$\eta = \frac{1}{\beta_1 E_e}, \quad (29)$$

q_e is derived from Eq. (22), and $\theta(x)$ is the Heaviside function.

If there were several eruption processes we should sum over them in order to get a resulting spectrum of positrons.

7. Evolution of the Positron Spectrum

7.1. Kinetic Equation

In order to estimate the flux in the $e^+ - e^-$ annihilation line we should calculate how many thermal positrons can be supplied by $p - p$ nuclear reactions under the influence of energy losses. Similar calculations were performed by Stecker (1969) who analyzed effects of energy losses only. Crannell et al. (1976) calculated the positron density produced in solar flares from the Fokker-Planck equation when positrons are injected at an energy of 1 MeV. Recently Guessoum et al. (2005) have studied the lives and deaths of positrons in the interstellar medium by using Monte Carlo simulations as well as a binary reaction rate approach. In our case we should use the generalized Fokker-Planck equation because positrons are injected at a relativistic energy of about 30 MeV.

The generalized Fokker-Planck equation, describing the particle distribution function f written in dimensionless variables is (see Dogiel 2000; Liang et al. 2002)

$$\frac{\partial f}{\partial t} + \frac{vn(\sigma_{an} + \sigma_{ce})}{\nu_0} f - q_e(p, \mathbf{r}) = \frac{1}{p^2} \frac{\partial}{\partial p} \left[\mathcal{A}(p) \frac{\partial f(p)}{\partial p} + \mathcal{B}(p) f \right], \quad (30)$$

where q_e describes the distribution of sources emitting fast particles. If we compare this equations with Eq.(9) for relativistic and subrelativistic cosmic rays we see that in order

to describe evolution of the positron spectrum from relativistic to thermal energies we include the terms in rhs which are responsible for the formation by Coulomb collisions of the equilibrium Maxwellian distribution with a given temperature of the background gas. The injection spectrum is given by the term q_e which is determined by the production of secondary electrons at energies above 30 MeV. As one can see from Fig. 5 the change in f at thermal energies implied by Eq. (30) is then a simple scaling with time, mediated by the ionization loss timescale. The charge-exchange annihilation processes describing by the cross-section σ_{ce} act for positrons as an absorbing boundary at low energies, especially for eV temperatures when the cross-section of annihilation increases by several orders of magnitude (Bussard et al. 1979; Guessoum et al. 2005). Therefore, for a constant production of positrons we have in the stationary case the annihilation rate of thermal positrons exactly equal to $\int q_e(p)p^2 dp$.

In our case this source function describes the production of positrons (shown in Fig. 4) with the rate $\sim 10^{41} e^+ s^{-1} GeV^{-1}$, the main part of which is concentrated near energies $E_{e^+} \sim 30 - 50$ MeV, and processes of positron annihilation are described by cross-sections σ_{ce} and σ_{an} (see section 6.1).

We define non-dimensional variables $p = p/\sqrt{mkT}$ and $t = \hat{t} \cdot \nu_0$, where the characteristic frequency ν_0 is

$$\nu_0 = \frac{2\pi\bar{n}_e c^2 r_e^2 m_e}{\sqrt{m_e k T_x}}, \quad (31)$$

where \bar{n}_e is the average electron number density, and r_e is the classical electron radius $r_e = e^2/m_e c^2$, $\bar{n}_e = 1 \text{ cm}^{-3}$ and $T_x = 2.5 \text{ eV}$, $\nu_0 \simeq 6.7 \times 10^{-12} \text{ s}^{-1}$.

In Eq. (30), \mathcal{B} describes the particle energy gain and loss and \mathcal{A} the momentum diffusion due to Coulomb collisions with background particles,

$$\mathcal{A}(p) = p^2 \left[- \left(\frac{dp}{dt} \right)_{ion} \frac{\gamma}{\sqrt{\gamma^2 - 1}} \sqrt{\frac{kT_x}{m_e c^2}} \right], \quad (32)$$

$$\mathcal{B}(p) = p^2 \left[- \left(\frac{dp}{dt} \right)_{ion} - \left(\frac{dp}{dt} \right)_{synIC} - \left(\frac{dp}{dt} \right)_{brem} \right], \quad (33)$$

where $\gamma = 1 + E(p)/m_e c^2$ is the Lorentz factor.

The dp/dt terms are rates of momentum loss due to ionization, synchrotron plus inverse Compton (IC) and bremsstrahlung emission respectively (e.g. Hayakawa 1969). The ionization loss term is

$$\left(\frac{dp}{dt} \right)_{ion} = -\frac{1}{p} \sqrt{p^2 + \frac{m_e c^2}{kT_x}} \frac{\gamma}{\sqrt{\gamma^2 - 1}} \times \left[\log \left(\frac{E(p) m_e c^2 (\gamma^2 - 1)}{h^2 \omega_p^2 \gamma^2} \right) + 0.43 \right], \quad (34)$$

where the plasma frequency $\omega_p = \sqrt{4\pi e^2 \bar{n}_e / m_e}$. The combined synchrotron and IC loss term is

$$\left(\frac{dp}{dt}\right)_{synIC} = -\frac{32}{9} \frac{1}{p} \sqrt{p^2 + \frac{m_e c^2}{kT_x} \frac{1}{\nu_0}} \times \frac{\pi r_e^2}{\sqrt{m_e kT_x}} [U_{cmb} + U_{mag}] \left(\frac{E(p)}{m_e c^2}\right)^2, \quad (35)$$

where U_{cmb} is the energy density of background photons, and U_{mag} is the magnetic energy density. The bremsstrahlung loss term is given by

$$\left(\frac{dp}{dt}\right)_{brem} = -\frac{1}{p} \sqrt{p^2 + \frac{m_e c^2}{kT_x} \frac{1}{\nu_0} \frac{E(p)}{m_e c^2} \frac{\bar{n}_e m_e c^2 e^2 r_e^2}{hc \sqrt{m_e kT_x}}} \left[\log \frac{2(E(p) + m_e c^2)}{m_e c^2} - \frac{1}{3} \right]. \quad (36)$$

The corresponding times of synchrotron+inverse Compton energy losses are shown in Fig. 1. The magnetic field strength is $H = 5 \times 10^{-6} \text{G}$ and the energy density of background photons $U_{cmb} = 1 \text{ eV cm}^{-3}$.

7.2. Numerical Calculations of Thermal Positron Numbers for the Case of Quasi-Stationary Production ($t < \tau_p \sim \tau_c$)

For calculations of the positron number at different times we used Eq. (30) describing the evolution of the positron spectrum in both the relativistic and nonrelativistic energy ranges. The dimensionless time $t = 1$ corresponds to $1.5 \times 10^{11} \text{ s}$. We include into the equation the process of positron annihilation whose cross-section at different energies is (see, e.g., Crannell et al. 1976)

$$\sigma_{an} = \frac{\pi r_e^2}{\gamma + 1} \left(\frac{\gamma^2 + 4\gamma + 1}{\gamma^2 - 1} \ln \left[\gamma + \sqrt{\gamma^2 - 1} \right] - \frac{\gamma + 3}{\sqrt{\gamma^2 - 1}} \right) \quad (37)$$

If the energy of positrons is below 1 keV and the medium is weakly ionized (as is the case at temperatures below 10 eV) then we should also include the charge-exchange annihilation, whose cross-section is :

$$\sigma_{ce} = 1.2 \times 10^{-15} \cdot \left(\frac{E_{e+}}{E_0} - 1 \right) \exp \left(1 - \frac{E_{e+}}{E_0} \right) \text{ cm}^2 \quad (38)$$

where E_{e+} is the positron energy and $E_0 = 6.8 \text{ eV}$. This equation was obtained from the experimental data of Sperber et al. (1992) with the approximation of Fatuzzo et al. (2001). The corresponding time of positron annihilation at different energies $\tau_{an} = (n\nu\sigma_{an})^{-1}$ is shown in Fig. 1 by a dotted line.

The production function of positrons is shown in Fig. 4. The injection function can be presented as $q_e(p, t) \propto Q_0(t)\theta(\bar{p} - \bar{p}_0)p^{-\gamma}$ where \bar{p}_0 corresponds to the maximum of the function $q_e(p)$ at the energy $E = 30$ MeV. We assume that annihilation processes take place in the extended medium surrounding the region, where the injected protons produce relativistic positrons. The time variation of the injection function is caused by catastrophic and ionization losses of protons. However, if we consider a time $t < \tau_p$ we can neglect time variations of the production function corresponding to the almost stationary case of positron production. We normalized the distribution function

$$\int_0^\infty p^2 dp q_e(p) = Q_0 \quad (39)$$

where Q_0 can be obtained from Fig. 4 and is about 10^{41} s^{-1} for $t < \tau_p$.

If we calculate from the kinetic equation (30) the number of thermal positrons annihilating in the eV temperature medium on the assumption that they are produced by the same relativistic protons which are responsible for the observed gamma-ray flux of $2 \cdot 10^{37} \text{ erg s}^{-1}$ then we obtain the value $2 \cdot 10^{41} \text{ e}^+ \text{ s}^{-1}$, which is two orders of magnitude less than necessary to explain the annihilation flux from the Galactic center. Therefore the stationary model fails to explain the data. Thus, in the framework of this model we cannot satisfy both conditions 1) and 5) presented at the end of Section 2.

8. Nonstationary Model of Positron Production

8.1. Positron Spectrum ($t > \tau_p \sim \tau_c$)

One of the solutions to this problem might be that in the past the positron production rate was much higher than follows from the current gamma-ray flux from the GC. Under this condition the production function of positrons calculated from Eq.(12) is an essential function of time, $q(p, t)$.

In Fig.5 the evolution of the positron spectrum calculated from Eq. (30) is shown for the parameters of the interstellar medium: the density $n = 1 \text{ cm}^{-3}$, the temperature $T = 2.5 \text{ eV}$, the magnetic field strength $H = 5 \times 10^{-6} \text{ G}$ and the energy density of background photons $U_{cmb} = 1 \text{ eV cm}^{-3}$.

The distribution function of the positrons injected at the initial stage at $\bar{p} > \bar{p}_0$ is shifted to the momentum region $\bar{p} < \bar{p}_0$ under the influence of Coulomb collisions that can be seen in Fig. 5 as a "bunch" of positrons propagating into the region of small momenta.

Later Coulomb collisions start to form the equilibrium Maxwellian distribution in the range $\bar{E} \leq 10^{-2}$ keV . At a subsequent point of time Coulomb collisions continue to form the equilibrium distribution and accumulate positrons in the thermal energy range, as can be seen in Fig. 5 as the increasing Maxwellian distribution. At the final stage when the source ceases to work the number of thermal positrons decreases because of annihilation (see Fig. 6).

We notice that the positron evolution and the number of thermal positrons depend on the background gas temperature, e.g. in the plasma with the temperature 100 eV we can produce a much larger amount of positrons because the annihilation cross-section in this medium is several orders of magnitude smaller than in a neutral gas (see Fig. 7).

Now we proceed to calculate the intensity of emission due to annihilation of positrons. Depending on the temperature and density of the ambient medium, electrons and positrons can annihilate either directly or via formation of positronium (Bussard et al. 1979; Guessoum et al. 1991, 2005).

The in-flight differential spectrum of the γ -rays produced by annihilation of a positron on the ambient electrons with density n_e (Aharonian and Atoyan 1981; Aharonyan and Atoyan 2000):

$$q_{an}(\varepsilon) = \frac{\pi r_e^2 c n_e}{\gamma_+ p_+} \left[\left(\frac{\varepsilon}{\gamma_+ + 1 - \varepsilon} + \frac{\gamma_+ + 1 - \varepsilon}{\varepsilon} \right) + 2 \left(\frac{1}{\varepsilon} + \frac{1}{\gamma_+ + 1 - \varepsilon} \right) - \left(\frac{1}{\varepsilon} + \frac{1}{\gamma_+ + 1 - \varepsilon} \right)^2 \right] \quad (40)$$

where $\gamma_+ = E_+/m_e c^2$ is the Lorentz-factor of the positron, $p_+ = \sqrt{\gamma_+^2 - 1}$ is the dimensionless momentum of positron and $\varepsilon = E/m_e c^2$ is the dimensionless photon energy. The energy spectrum of in-flight annihilation

$$N_{an}(\varepsilon) = \int_{\gamma}^{\infty} q_{an}(\gamma_0, \varepsilon) n_e(\varepsilon) d\gamma_0 \quad (41)$$

The lower integration limit can be obtained from the kinetic equations and equals

$$\gamma(\varepsilon) = \frac{\varepsilon^2 + (\varepsilon - 1)^2}{2\varepsilon - 1} \quad (42)$$

The energy spectrum of annihilation photons produced by the charge-exchange process is (Bussard et al. 1979)

$$N_{ce}(\varepsilon) = \int_E^{\infty} dE_0 n_H n_e(E_0) \sigma_{ce}(E_0) v \div [(E_0 - 6.8eV)(E_0 - 6.8eV + 4\varepsilon)]^{1/2} \quad (43)$$

where $E = (\varepsilon - \varepsilon_0)^2 / \varepsilon + 6.8 \text{ eV}$, ε_0 - the rest mass of positronium, n_H - the density of neutral hydrogen.

To fit the INTEGRAL data (Churazov et al. 2005), shown at Fig. 8, we used the following medium parameters: plasma temperature 2.5 eV, plasma density 1 cm^{-3} , degree of ionization 5% (see, e.g., Kaplan and Pikelner 1979). The plasma temperature affects the width of the annihilation line. In order to fit the INTEGRAL data for energies at and below 511 keV we need a temperature in the region 2-5 eV.

The line emission at these temperatures is due to the two photon decay of the charge-exchange process. The emission below 511 keV is generated by three photon decay of positronium. The process of in-flight annihilation in a low temperature medium is negligible because the time for thermalization in this medium is smaller than the characteristic time of the in-flight annihilation. This process is essential in the hot component of the interstellar medium, about 20% of which is filled by a hot plasma with the parameters $T = 100 \text{ eV}$ and $n = 3 \times 10^{-3} \text{ cm}^{-3}$. However, as one can see from Fig. 9 the flux of the annihilation line produced in the hot interstellar plasma by in-flight annihilation is negligible in comparison with emission in a cold plasma.

The temporal variations of the gamma-ray and the annihilation fluxes are shown in Fig. 10. The maximum of the fluxes are taken as unity. We see that the gamma-ray flux is always decreasing with time, while the annihilation flux reaches its maximum a long time after the proton eruption ($\sim 3 \times 10^{14} \text{ s}$) and then gradually decreases. We can estimate the necessary input proton energy without going into the technical calculation details. The current observed energy flux of gamma-rays is $2 \times 10^{37} \text{ erg s}^{-1}$ and the current annihilation rate of thermal positrons is $10^{43} \text{ positron s}^{-1}$, corresponds to a higher proton collision rate in the past. From Fig. 10, one can see that this situation is realized if we are observing these fluxes at a time $t > \tau_p$ when the current gamma-ray intensity is at least three order of magnitude less than its maximum, while the current annihilation flux falls from its maximum value by less than one order of magnitude (just because of the delay effect). In this case, the necessary input proton energy is at least $\sim 10^{55} \text{ erg}$. Of course, this estimate sensitively depends on the number density. Even if we take the average density of the gas in the bulge as high as $n = 100 \text{ cm}^{-3}$ (see Section 4) we get a value of the energy necessary to produce the gamma-ray and annihilation fluxes about $W_p \sim 10^{53} \text{ erg}$. This amount of energy may be able to be supplied by a very massive star accreting onto the black hole (see Eq. 5) or by extracting the rotation energy of the black hole (see Eq. 6). However, we may not be able to obtain a distribution of the annihilation line extending to several hundred pc from the GC because the characteristic length of diffusion propagation is about 100 pc for this high gas density. Thus, in the framework of this model we have problems with the conditions 2)

or 4) from Section 2. Nevertheless, we conclude that this model is marginally acceptable if a $50 M_{\odot}$ massive star was captured by the black hole about hundred million years ago.

9. Spatially Non-Uniform Model ($\tau_p < t \sim \tau_c$)

To solve the possible problem of energy excess we take into account that the background gas is heterogeneously distributed in the bulge (see Section 4). According to Jean et al. (2005) hydrogen gas in the nuclear bulge is trapped in small high density molecular clouds. Penetration of cosmic rays into molecular clouds was analyzed in a number of papers (see, e.g., Cesarsky and Voelk 1978; Dogiel and Sharov 1985; Padoan and Scalo 2005). From the EGRET observations it is known that GeV cosmic ray protons freely penetrate into molecular clouds (Digel et al. 1999) while it is almost unknown how MeV electrons interact with the clouds. However, Skilling and Strong (1976) showed that the flux of cosmic rays below a few hundred MeV might be completely excluded from molecular clouds.

In our case it means that relativistic protons propagate in the medium with the average gas density about $n=30 - 1000 \text{ cm}^{-3}$ (depending on their propagation distance from the bulge center) while the secondary positrons ejected from the clouds propagate in the intercloud medium only, where the average gas density is about $n \simeq 1 - 10 \text{ cm}^{-3}$.

For protons it means that they fill the region of a radius $< 100 \text{ pc}$ (if the diffusion coefficient equals the average in the Disk, $D \sim 10^{27} \text{ cm}^2\text{s}^{-1}$) during their lifetime $\tau_p \sim (1 - 5) \times 10^{13} \text{ s}$ while electrons can fill a sphere of radius $\sim 400 \text{ pc}$ over the period of time of their Coulomb cooling ($\sim 3 \times 10^{14} \text{ s}$ for $n = 1 \text{ cm}^{-3}$).

The time variations of the gamma-ray and annihilation emission are shown in Fig. 11 for an average density for protons $n = 30 \text{ cm}^{-3}$. As is to be expected the gamma-ray flux drops rapidly from its initial value while the annihilation flux reaches its maximum $\sim 3 \times 10^{14} \text{ s}$ after the eruption. The energy of relativistic protons necessary to get the peak production of thermal positrons of about $10^{43} \text{ e}^+\text{s}^{-1}$ is about $7 \cdot 10^{53} \text{ erg}$. The energy in relativistic protons changes weakly if we increase further the gas density. Thus, for a density $n = 100 \text{ cm}^{-3}$ the necessary energy of the protons is $5 \cdot 10^{53} \text{ erg}$. These injected proton energies are compatible with the estimates in Eq.(5) or Eq.(6) for a massive star capture.

Besides, if the average density of the gas in the medium traversed by positrons is a little bit higher than 1 cm^{-3} (e.g, 3 cm^{-3}) than we obtain slightly smaller values for the thermalization time ($\sim 10^{14}\text{s}$) as well as the necessary energy output of protons ($\sim 10^{53} \text{ erg}$) that makes our estimates even more acceptable.

Then, we can assume that the gamma-ray and the annihilation fluxes from the Galactic center belong to different accretion events. Gamma-rays were generated relatively recently ($\sim 10^{13}$ s ago) when a one solar mass star was captured by the black hole. Indeed the necessary amount of energy in injected protons is about $\gtrsim 10^{51} - 10^{52}$ erg (see Section 5). In this respect it is clear why this emission was observed by EGRET as point-like. The average length of proton propagation is $\lesssim 100$ pc for the diffusion coefficient $D = 10^{27} \text{ cm}^2\text{s}^{-1}$. If the annihilation line emission was produced $\sim 10^{14}$ s ago by a previous event of a $30 M_\odot$ star capture, with an energy release of $\gtrsim 10^{53}$ erg in protons, then it appears as an extended source long after the time when the gamma-ray emission produced by this capture died out. Thus, this model satisfies the conditions formulated in Section 2 though the annihilation and gamma-ray fluxes observed from the GC are not connected with each other in this case.

10. Continuous stellar captures

In the framework of the non-uniform model we can estimate the minimum energy at relativistic protons in order to produce in the current time the thermal positron rate of about $10^{43} \text{ e}^+\text{s}^{-1}$ and not contradict the gamma-ray observations. We remember that the present gamma-ray flux from GC is about $2 \cdot 10^{37} \text{ erg}^{-1}$ and it is seen as a point-like object. We remember also that the gas distribution is unknown but that the main part of the gas is concentrated inside the central region of the bulge where its density is as high as $\sim 1000 \text{ cm}^{-3}$ (see Jean et al. 2005). If relativistic protons freely penetrate into the clouds the average density $n \sim 1000 \text{ cm}^{-3}$. We define this density as n_{pp} .

The diffuse gas is distributed in the intercloud medium with an average density of 10 cm^{-3} and it may reach at the central regions the value of $30 - 60 \text{ cm}^{-3}$. If positrons do not penetrate into the cloud then the gas density of the medium in which positrons are cooled down by the Coulomb collisions is determined by these values. Below, we define this gas density as n_{cc} . Let us estimate the minimum energy of primary protons necessary to produce the annihilation flux as a function of n_{pp} and n_{cc} .

In the framework of the nonuniform model the initial energy of protons necessary to produce the annihilation emission depending on n_{pp} and n_{cc} is varying in the following way: It is clearly seen that when we increase the value of n_{pp} the output energy of protons decreases because the production rate of relativistic positrons is proportional to the gas density

$$F_{e^+} = \int N_p(E_p) \sigma_{pp} n_{pp} dE_p \quad (44)$$

However as follows from Table 1 the proportionality between W_p and n_{pp} is not linear as it would seem from Eq.(44). From Eq.(44) one can see that the higher the density n_{pp} the

Table 1: Injected Proton Energy

$n_{pp}(\text{cm}^{-3})$	$n_{cc}(\text{cm}^{-3})$	$W \text{ (erg)}$
1	1	10^{55}
30	1	$7 \cdot 10^{53}$
100	1	$5 \cdot 10^{53}$
100	10	$2 \cdot 10^{53}$
1000	1	$2 \cdot 10^{53}$
1000	10	$1.5 \cdot 10^{53}$
1000	30	$4.5 \cdot 10^{52}$
1000	60	$3 \cdot 10^{52}$

shorter is the injection impulse of positrons which is determined by the lifetime of protons $\tau_p = n_{pp}\sigma_{pp}c$. The necessary energy output of protons as a function of the ratio n_{pp}/n_{cc} is shown in Fig. 12. In the figure we take the density $n_{cc} = 1 \text{ cm}^{-3}$ and W_0 is the proton energy when $n_{pp}/n_{cc} = 1$. The variation of the proton injected energy W_p can easily be understood from the solution of the diffusion equation. When $n_{pp}/n_{cc} = 1$ we have $\tau_p \gtrsim \tau_c$ and the energy W_p at this density for a fixed flux of thermal positrons at the level $F_{e^+} \sim 10^{43} \text{ e}^+ \text{ s}^{-1}$ is of the order of $W_p \propto \tau_p \cdot F_e^+$ i.e it decreases as $W \propto 1/n_{pp}$. However when $n_{pp} \gg n_{cc}$ the impulse of proton injection is very short $\tau_p \ll \tau_c$ (almost delta-function injection) and we obtain $W_p \propto \tau_c \cdot F_e^+$, i.e W_p is independent of n_{pp} as one clearly sees in Fig. 12. The time τ_c cannot be too short otherwise the gamma-ray flux would not drop down below the observed gamma-ray flux from the GC (see Fig. 11). Variations of the gamma-ray flux for a fixed annihilation flux of thermal positrons of $10^{43} \text{ ph s}^{-1}$ as a function of the ratio n_{pp}/n_{cc} is shown in Fig. 13. From this figure we see that this ratio cannot be below $n_{pp}/n_{cc} = 17$ otherwise the peaks of gamma-rays and the annihilation emission are so close to each other that the flux of gamma-rays does not have enough time to drop below the observed limit.

From this restriction we conclude that the injected proton energy cannot be less than $\sim 3 \times 10^{52} \text{ erg}$ even for $n_{pp} = 1000 \text{ cm}^{-3}$ while $n_{cc} = 60 \text{ cm}^{-3}$. This gives the average distance of proton propagation by diffusion of about 20 pc and about 100 pc for positrons during their lifetime, which is less than necessary, but the diffusion coefficient may be spatially dependent such that it gives a more extended positron spatial distribution. Under this assumption even the capture of $1 M_\odot$ star can give the necessary energy in protons as follows from Eq.(5) or Eq.(6), and the process of annihilation emission is not an exceptional event as we had in the previous models when a massive star capture was needed to supply the necessary energy in relativistic protons.

Since there are so many stars at the GC, there is very good reason to believe that the capture of stars can continuously take place from time to time. If there are several successive eruptions near the black hole then the annihilation flux is fluctuating near a certain level of emission as is shown in Fig. 14. In the calculations we take $n_{cc} = 60 \text{ cm}^{-3}$ and $n_{pp} = 1000 \text{ cm}^{-3}$ which give $\tau_c \sim 5 \times 10^{12} \text{ s}$ and $\tau_p \sim 7 \times 10^{11} \text{ s}$ respectively. The time between two successive eruption equals $\sim 8 \times 10^{12} \text{ s}$. When the variations of the energy fluxes of gamma-rays and the photon flux of the annihilation emission are normalized relative to their maximum their values, which for gamma-rays is $3 \times 10^{39} \text{ erg s}^{-1}$ and for the annihilation flux is $10^{43} \text{ ph s}^{-1}$, the average injected proton energy is $\sim 8 \times 10^{52} \text{ erg}$.

11. TeV Gamma-Rays

It is very interesting to find other confirmations of eruption processes from observed data. In this respect, the new data in the TeV gamma-ray range are of strong interest.

Recently, TeV γ -ray emission at a luminosity higher than $10^{35} \text{ ergs s}^{-1}$ from the direction of the galactic center has been reported by three independent groups, Whipple (Kosack et al. 2004), CANGAROO (Tsuchiya et al. 2004), and HESS (Aharonian et al. 2004). The most plausible candidates suggested for this emission include the black hole Sgr A* (Aharonian and Neronov 2005b) and the compact and powerful young supernova remnant (SNR) Sgr A East (Crocker et al. 2005). The angular scale of the TeV source was determined by HESS to be about a few arc-minutes, indicating that this γ -ray source is located in the central $\sim 10 \text{ pc}$ region (Aharonian et al. 2004). The gamma-ray spectrum observed by HESS can be described by $F(E_\gamma) = (2.5 \pm 0.21) \times 10^{-12} E_\gamma^{-2.21} \text{ ph}/(\text{cm}^2 \text{ s TeV})$, which is consistent with decay of π^0 produced by p-p collisions with the initial spectrum of the injection protons as $Q(E) = Q_0 E^{-2.2} \exp(-E/E_0)$, where the cutoff energy is $E_0 = 10^{15} \text{ eV}$ (Aharonian and Neronov 2005b). In comparing with the diffuse gamma-ray spectrum detected by EGRET (cf. Eq. 2), the TeV spectrum is flatter. If both GeV and TeV gamma-rays result from the decay of π^0 which are produced by p-p collisions, it appears that these two different energy gamma-ray spectra must be produced by two different groups of protons. Furthermore, the protons responsible for the diffuse GeV gamma-ray emission must be ejected by Sgr A* much earlier than those responsible for the TeV gamma-rays because their angular sizes are so much different. In fact, these two requirements are consistent with our model considered here, i.e. the galactic black hole is activated by capturing stars.

If we assume that positrons are produced via $p-p$ collisions and these protons are emitted from the galactic black hole, by taking the typical diffusion coefficient ($D \sim 10^{27} \text{ cm}^2 \text{ s}^{-1}$), we can estimate that these relativistic protons should be emitted at a earlier time $t_{diff} \sim$

$\frac{(0.5kpc)^2}{6 \times 10^{27} cm^2/s} \sim 3 \times 10^{14}s$, which is consistent with the requirement of the annihilation line. Again if we assume that TeV photons also result from the decay of neutral pions produced by p-p collisions and that these protons are emitted from the galactic black hole, then taking the same diffusion coefficient, we obtain that these protons are emitted at a earlier time $t_{diff} \sim \frac{(10pc)^2}{6 \times 10^{27} cm^2/s} \sim 5 \times 10^3 years$, which is shorter than the typical capture time of a main sequence star by a factor of 60. However, $D \sim 10^{27} cm^2 s^{-1}$ is the mean diffusion coefficient for the Galaxy obtained by cosmic ray measurements (Berezinskii et al. 1990). The diffusion coefficient near the Galactic center can be significantly smaller. For example, the Bohm diffusion time can be estimated as $t_{Bohm} \sim (\frac{\lambda}{r_L})^2 \frac{r_L}{6c}$ where λ is the diffusion distance, $r_L \approx E_p/eB$ is the Larmor radius, E_p is the proton energy for producing TeV photons and B is the local magnetic field. Using $\lambda \sim 10$ pc, $E_p \sim 3TeV$ and $B \sim 10^{-5}G$, we obtain $t_{Bohm} \sim 2 \times 10^5 years$, which is similar to the requirement of the continuous capture model. Taking the observed TeV luminosity $\sim 10^{35} erg/s$ that implies the injected proton energy must be at least $\sim 10^{51} erg$ (Aharonian et al. 2004), which is consistent with our estimation of energy release for capturing a $1M_\odot$ star (cf. Eq. 5). Furthermore, the injected proton index for TeV gamma-rays is ~ 2.2 but the injected proton index for the diffuse GeV gamma-rays is ~ 2.6 in our model calculation. It appears that they have different origins. However, this discrepancy can be explained by the following possibilities. (1) The simplest explanation may be that the injected proton spectrum can vary from injection to injection. (2) The most realistic explanation should be due to propagation effects and leakage effects which occur in the Galaxy where the injection spectrum with the spectral index as $Q(E) \propto E^{-(2.0-2.2)}$ steepens due to energy variations of the spatial diffusion coefficient, as $D \propto E^{-0.6}$ (see Berezinskii et al. 1990).

Lu et al. (2005) have suggested that the TeV emission from the GC resulting from a powerful relativistic proton jet emitted by Sgr A* about $\sim 10^4 years$ ago, which result from the capture of a red giant star. However, their conclusion is based on a comparison of the diffusion length of the relativistic protons with the upper limit on the size of the TeV source. It should be noticed that the lack of information beyond 10 pc does not mean an absence of such an extended component. Detection of an extended region with a weaker signal is very difficult. In this model we predict that when more TeV data are available the TeV spectrum may show a spatial dependence. In particular, the TeV signals from a more extended region should exhibit a steeper spectrum if the propagation and leakage effects are indeed the origins of the spectral discrepancy between GeV gamma-rays and TeV gamma-rays.

12. Discussion

We suggest that the capture of stars by the Galactic black hole is a natural energy mechanism for providing relativistic protons with a typical energy of $\sim 10^{52-53}$ erg. An essential point of our analysis is the non-stationary processes and the non-uniform density conditions of emission regions.

The duration of energy emission as well as of the existence of relativistic protons after accretion is much shorter than the mean interval between two accretion events. Once ejected by the central black hole, relativistic protons propagate by diffusion into the interstellar medium surrounding the hole occupying a more and more extended region around the Galactic Center. Collisions of these protons with the ambient gas result in secondary gamma-rays and relativistic positrons with energies $E > 30$ MeV. The total gamma-ray flux is almost constant during the lifetime of the protons but then it decays exponentially with the characteristic time dependent on the gas density. Secondary relativistic positrons produced immediately via $p-p$ collisions are almost unseen at the first stage after the eruption because the annihilation flux of fast positrons is almost negligible. These positrons are cooled down by Coulomb collisions with the ambient gas with the characteristic time for Coulomb collisions. Only when positrons reach an energy of about several eV they effectively annihilate in the warm neutral and ionized phases of the interstellar medium where the cross-section for annihilation increases by several orders of magnitude (see Bussard et al. 1979; Guessoum et al. 1991, 2005) and results in an increase of the annihilation emission. The maximum of the annihilation emission is reached long after the eruption moment. At that time positrons fill an extended region around the Galactic center by diffusion and therefore in all cases the annihilation emission can be seen as an extended region around the Galactic center, the annihilation flux is never seen as a point-like central source. On the other hand, the high energy gamma-rays are produced from the very beginning of the eruption and can be seen in the first stages after the eruption as a point-like source.

Our calculations show that it is marginally possible that the gamma-rays coming from the GC and the annihilation emission belong to the same eruption process provided the injected proton energy is $\sim 10^{54}$ erg, this might be possible theoretically if we take model parameters to their extreme values. An alternative assumption that the currently observed gamma-rays from the GC and the currently observed annihilation emission belong to at least two different injections seems to be more attractive. The first one belong to a recent capture of a one solar mass star with the injected energy of about 3×10^{51} erg while the second one is a consequence of a previous capture of a much more massive star with an energy release as high as 10^{53} erg. This does not contradict estimations from theoretical models if we assume capture of a massive star.

Furthermore, if processes of secondary particle production occur very close to the GC where the gas density is about 1000 cm^{-3} then even a $1 M_{\odot}$ star capture can provide the necessary energy of protons, which is in this case $\sim 3 \cdot 10^{52}$ erg. The GC is a region with a high concentration of stars, the capture of a star should continue to take place from time to time. Although the characteristic capture time scale is not known, TeV emission from the GC suggests that it should be $> 10^5 \text{ yr}$. If this is true, assuming the positrons cannot penetrate the cloud, so that the cooling time is longer than the $p - p$ collision time, our calculations indicate that the positron annihilation rate is more or less constant whereas the current gamma-ray flux is measured somewhere between two proton injection events. This naturally explains why the annihilation rate is about two orders of magnitude higher than follows from the current emission rate of gamma-ray photons.

The authors are grateful A.Aharonyan, E.Churazov, Y.F. Huang, Y. Lu and the anonymous referee for very useful discussions and comments. We also thank P.K. MacKeown for this critical reading of the manuscript. VAD is also grateful to T. Harko and Anisia Tang for their consultations in carrying out the numerical calculations. This work is supported by a RGC grant of Hong Kong Government and by the grant of a President of the Russian Federation "Scientific School of Academician V.L.Ginzburg".

REFERENCES

- Aharonian, F.A. and Atoyan, A.M. 1981, Physics Letters B, 99, 301
- Aharonyan, F.A., and Atoyan, A. M. 2000, A&A, 362, 937
- Aharonian, F.A., et al. 2004, A&A, 425, L13
- Aharonian, F., and Neronov, A. 2005a, astro-ph/0503354
- Aharonian, F., and Neronov, A. 2005b, ApJ, 619, 306
- Aharonian, F.A., et al. 2006, Nature, 439, 695
- Atoyan, A. M. 1992, A&A, 257, 476
- Bahcall, J. N., and Wolf, R. A. 1976, ApJ, 209, 214
- Berezinskii, V. S., Bulanov, S. V., Dogiel, V. A., Ginzburg, V. L., and Ptuskin, V. S. 1990, *Astrophysics of Cosmic Rays*, ed. V.L.Ginzburg, (North-Holland, Amsterdam)

- Blandford, R.D., and Znajek, R.L. 1977, MNRAS, 179, 433
- Boehm, C., Hooper, D., Silk, J., Casse, M., and Paul, J. 2004, PhRvL, 92, 1301
- Bouchet, L., Roques, J. P., Mandrou, P., Strong, A., Diehl, R., Lebrun, F., and Terrier, R. 2005, ApJ, 635, 1103
- Breitschwerdt, D.; McKenzie, J. F.; Voelk, H. J. 1993, A&A, 269, 54
- Brunetti, G., and Blasi, P. 2005, MNRAS, 363, 1173
- Buckley, J.H., et al. 1997, Proc. 25th Int. Cosmic Ray Conf. (Durban), 237
- Bussard, R.W., Ramaty, R., and Drachman, R.J. 1979, ApJ, 228, 928
- Casse, M., Cordier, B., Paul, J., and Schanne, S. 2004, ApJ, 602, L17
- Cesarsky, C. J., and Voelk, H. J. 1978, A&A, 70, 367
- Chan, K.-W., and Lingenfelter, R. E. 1993, ApJ, 405, 614
- Cheng, K.S., and Lu, Y. 2001, MNRAS, 320, 235
- Cheng, L.X., Leventhal, M., Smith, D.M., Purcell, W. R.; Tueller, J.; Connors, A.; Dixon, D.; Kinzer, R. L.; and Skibo, J. G. 1997, ApJ, 481, L43
- Churazov, E.; Gilfanov, M.; Sunyaev, R.; Khavenson, N.; Novikov, B.; Dyachkov, A.; Kremnev, R.; Sukhanov, K.; Cordier, B.; Paul, P.; Laurent, P.; Claret, A.; Bouchet, L.; Roques, J. P.; Mandrou, P.; and Vedrenne, G. 1994, ApJS, 92, 381
- Churazov, E., Sunyaev, R., Sazonov, S., Revnivtsev, M., and Varshalovich, D. 2005, MNRAS, 357, 1386
- Crannell, C.J., Joyce, G., Ramaty, R., and Werntz, C. 1976, ApJ, 210, 582
- Crocker, Roland M.; Fatuzzo, Marco; Jokipii, J. R.; Melia, Fulvio; Volkas, Raymond R. 2005, ApJ, 622, 892
- Daniel, R.R. and Stephens, S.A., 1975, Space Science Reviews, 45, 158
- Dermer, C.D. 1986 A&A, 157, 223
- Dermer, C.D., and Murphy R. J. 2001, In: Exploring the gamma-ray universe. Proceedings of the Fourth INTEGRAL Workshop, Alicante, Spain. Editor: B. Battarick, Scientific editors: A. Gimenez, V. Reglero & C. Winkler. ESA SP-459, Noordwijk: ESA Publications Division, ISBN 92-9092-677-5, p. 115

- Digel, S. W., Aprile, E., Hunter, S. D., Mukherjee, R., and Xu, F. 1999, ApJ, 520, 196
- Dirac, P. A. M. 1930, Proc.Camb.Phil.Soc. 26, 361
- Dogiel, V. A. 2000, A&A, 357, 66
- Dogiel, V. A., and Sharov, G. S. 1985, Soviet Astronomy Letters, 11, 346
- Dogiel, V.A., and Sharov, G.S. 1990, A&A, 229, 259
- Falcke, H., and Biermann, P.L. 1999, A&A, 342, 49
- Fatuzzo, M., Melia, F., and Rafelski, J. 2001, ApJ, 549, 293
- Fatuzzo, M., and Melia, F. 2003, ApJ, 596, 1035
- Ferrière, K. 2001, Rev.Mod.Phys., 73, 1031
- Foglizzo, T., and Ruffert, M. 1997, A&A, 320, 342
- Ginzburg, V.L. 1989, *Applications of Electrodynamics in Theoretical Physics and Astrophysics*, Gordon and Breach Science Publication.
- Ginzburg, V.L., and Syrovatskii 1964, *The Origin of Cosmic Rays*, Macmillan, New York
- Gratton, L. 1972, Ap&SS, 16, 81
- Guessoum, N., Ramaty, R., and Lingenfelter, R. E. 1991, ApJ, 378, 170
- Guessoum, N., Jean, P. and Gillard, W. 2005, A&A, 436, 171
- Halpern, J.P., Gezari, S. and Komossa, S. 2004, ApJ, 604, 572
- Hayakawa, S. 1964, *Cosmic Ray Physics*, Interscience Monographs
- Hayakawa, S., Okuda, H., Tanaka, Y., and Yamamoto, Y. 1964, Progr. Theor.Phys.Suppl. (Japan) 30, 153
- Heinz, S., and Sunyaev, R. 2002, A&A, 390, 751
- Heitler, W. 1960, *The Quantum Theory of Radiation*, Oxford University Press, London
- Hills, J.G. 1975, Nature, 254, 295
- Jean, P., Knodlseder, J., Gillard, W., Guessoum, N., Ferriere, K., Marcowith, A., Lonjou, V., and Roques, J. P. 2006, A&A, 445, 579

- Johnson, W.N., III, Harnden, F.R., and Haymes, R.C. 1972, ApJ, 172, L1
- Kaplan, S.A, and Pikelner, S.B. 1979, *The Physics of the Interstellar Medium*, Nauka
- Kardashev, N. S. 2001, MNRAS, 326, 1122
- Koyama, K., Maeda, Y., Sonobe, T., Takeshima, T., Tanaka, Y., and Yamauchi, S., 1996, PASJ, 48, 249
- Knoedlseder, J.; Jean, P.; Lonjou, V.; Weidenspointner, G.; Guessoum, N.; Gillard, W.; Skinner, G.; von Ballmoos, P.; Vedrenne, G.; Roques, J.-P.; Schanne, S.; Teegarden, B.; Schoenfelder, V.; and Winkler, C. 2005, A&A, 441, 513
- Kosack, K., Badran, H. M.; Bond, I. H.; Boyle, P. J.; Bradbury, S. M.; Buckley, J. H.; Carter-Lewis, D. A.; Celik, O.; Connaughton, V.; Cui, W.; Daniel, M.; D’Vali, M.; de la Calle Perez, I.; Duke, C.; Falcone, A.; Fegan, D. J.; Fegan, S. J.; Finley, J. P.; Fortson, L. F.; Gaidos, J. A.; Gammell, S.; Gibbs, K.; Gillanders, G. H.; Grube, J.; Gutierrez, K.; Hall, J.; Hall, T. A.; Hanna, D.; Hillas, A. M.; Holder, J.; Horan, D.; Jarvis, A.; Jordan, M.; Kenny, G. E.; Kertzman, M.; Kieda, D.; Kildea, J.; Knapp, J.; Krawczynski, H.; Krennrich, F.; Lang, M. J.; Le Bohec, S.; Linton, E.; Lloyd-Evans, J.; Milovanovic, A.; McEnery, J.; Moriarty, P.; Muller, D.; Nagai, T.; Nolan, S.; Ong, R. A.; Palladini, R.; Petry, D.; Power-Mooney, B.; Quinn, J.; Quinn, M.; Ragan, K.; Rebillot, P.; Reynolds, P. T.; Rose, H. J.; Schroedter, M.; Sembroski, G. H.; Swordy, S. P.; Syson, A.; Vassiliev, V. V.; Wakely, S. P.; Walker, G.; Weekes, T. C.; and Zwerink, J. 2004, ApJ, 608, L97
- Koyama Katsuji, Maeda Yoshitomo, Sonobe Takashi, Takeshima Toshiaki, Tanaka Yasuo, and Yamauchi Shigeo 1996, PASJ, 48, 249
- LaRosa T.N. et al. 2005, ApJ, 626, 23
- Le, Truong and Becker, P. A. 2004, ApJ, 617, L25
- Leventhal, M., NacCallum, C. J., and Stang, P. D. 1978, ApJL, 225, L11
- Liang, H., Dogiel, V. A., and Birkinshaw, M. 2002, MNRAS, 337, 567
- Lightman A.P., and Shapiro, S.L. 1977, ApJ, 211, 244
- Liu, S., Petrosian, V., and Melia, F. 2004, ApJ, 611L, 101
- Lu, Y., Cheng, K.S., and Huang, Y.F. 2005, ApJ, in press

- Mayer-Hasselwander, H. A.; Bertsch, D. L.; Dingus, B. L.; Eckart, A.; Esposito, J. A.; Genzel, R.; Hartman, R. C.; Hunter, S. D.; Kanbach, G.; Kniffen, D. A.; Lin, Y. C.; Michelson, P. F.; Muecke, A.; von Montigny, C.; Mukherjee, R.; Nolan, P. L.; Pohl, M.; Reimer, O.; Schneid, E. J.; Sreekumar, P.; and Thompson, D. J. 1998 A&A, 335, 161
- Melia, F.; Yusef-Zadeh, F.; and Fatuzzo, M. 1998, ApJ, 508, 676
- Melrose, D.B. 1980, *Plasma Astrophysics. Nonthermal processes in diffuse magnetized plasma*, New York: Gordon and Breach
- Muno, M. P., Baganoff, F. K., Bautz, M. W., Feigelson, E. D., Garmire, G. P., Morris, M. R., Park, S., Ricker, G. R., and Townsley, L. K. 2004, ApJ, 613, 326
- Ore, A., and Powell, J. L. 1949, Phys.Rev, 75, 1696
- Padoan, P., and Scalo, J. 2005, ApJ, 624, L97
- Phinney, E. S. 1989, Nature, 340, 595
- Rees, M.J. 1988, Nature, 333, 523
- Sirota, V. A., Il'yin, A.S., Zybin, K.P. and Gurevich, A.V. 2005, JETP, 127, 331
- Skilling, J., and Strong, A. W. 1976, A&A, 53, 253
- Sperber, W., Becker, D., Lynn, K.G., Raith, W., Schwab, A., Sinapius, G., Spicher, G., and Weber, M. 1992, PhRvL, 68, 3690
- Stecker, F. W. 1969, Astrophys.Sp.Sci. 3, 579
- Stephens, S. A.; and Badhwar, G. D. 1981 Ap&SS, 76, 213
- Strong, A. W.; Moskalenko, I. V.; and Reimer, O. 2000 ApJ, 537, 763
- Syer, D., and Ulmer, A. 1999 MNRAS, 306, 35
- Syrovatskii S.I. 1959, Sov.Astron., 3, 22
- Teegarden, B. J.; Watanabe, K.; Jean, P.; Knodlseder, J.; Lonjou, V.; Roques, J. P.; Skinner, G. K.; von Ballmoos, P.; Weidenspointner, G.; Bazzano, A.; Butt, Y. M.; Decourchelle, A.; Fabian, A. C.; Goldwurm, A.; Gudel, M.; Hannikainen, D. C.; Hartmann, D. H.; Hornstrup, A.; Lewin, W. H. G.; Makishima, K.; Malzac, A.; Miller, J.; Parmar, A. N.; Reynolds, S. P.; Rothschild, R. E.; Schonfelder, V.; Tomsick, J. A.; and Vink, J. 2005, ApJ, 621, 296

- Tsuchiya, K., Enomoto, R.; Ksenofontov, L. T.; Mori, M.; Naito, T.; Asahara, A.; Bicknell, G. V.; Clay, R. W.; Doi, Y.; Edwards, P. G.; Gunji, S.; Hara, S.; Hara, T.; Hattori, T.; Hayashi, Sei.; Itoh, C.; Kabuki, S.; Kajino, F.; Katagiri, H.; Kawachi, A.; Kifune, T.; Kubo, H.; Kurihara, T.; Kurosaka, R.; Kushida, J.; Matsubara, Y.; Miyashita, Y.; Mizumoto, Y.; Moro, H.; Muraishi, H.; Muraki, Y.; Nakase, T.; Nishida, D.; Nishijima, K.; Ohishi, M.; Okumura, K.; Patterson, J. R.; Protheroe, R. J.; Sakamoto, N.; Sakurazawa, K.; Swaby, D. L.; Tanimori, T.; Tanimura, H.; Thornton, G.; Tokanai, F.; Uchida, T.; Watanabe, S.; Yamaoka, T.; Yanagita, S.; Yoshida, T.; and Yoshikoshi, T. . 2004, ApJ, 606, L115
- Weidenspointner, G., Knoedlseder, J., Jean, P. et al. 2005, SF2A-2005: Semaine de l’Astrophysique Francaise, Strasbourg, France, (eds. F. Casoli, T. Contini, J.M. Hameury and L. Pagani), EdP-Sciences, Conference Series, p. 471
- Weidenspointner, G., Shrader, C. R., and Knoedlseder, J. 2006, astro-ph/0601673
- Zheleznyakov V. V., and Belyanin, A. A. 1994 A&A, 287, 782

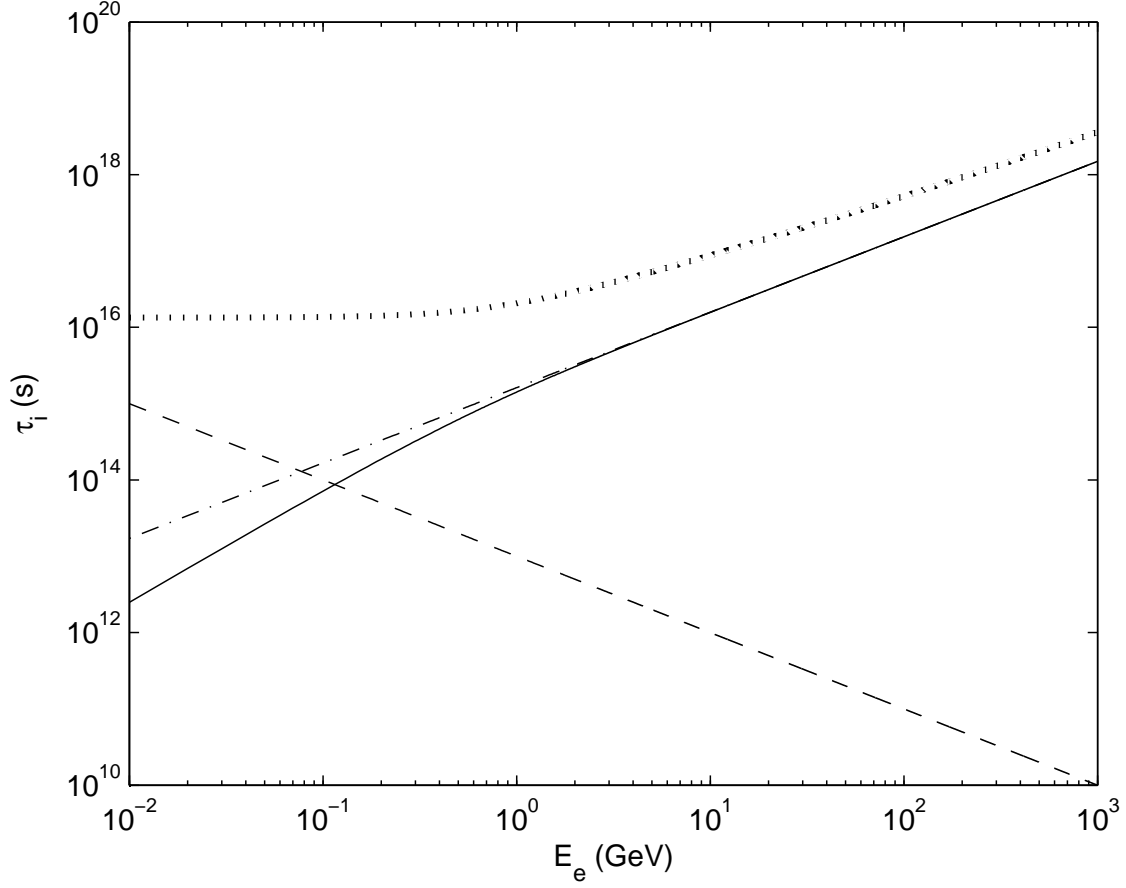


Fig. 1.— Variations of life-times due to ionization losses when $n = 1 \text{ cm}^{-3}$: for electrons (dashed-dotted line) and protons (solid line), due to synchrotron ($H = 5 \times 10^{-6} \text{ G}$) and inverse Compton ($w_{ph} = 1 \text{ eV cm}^{-3}$) energy losses for relativistic electrons (dashed line), and due to direct annihilation (dotted line).

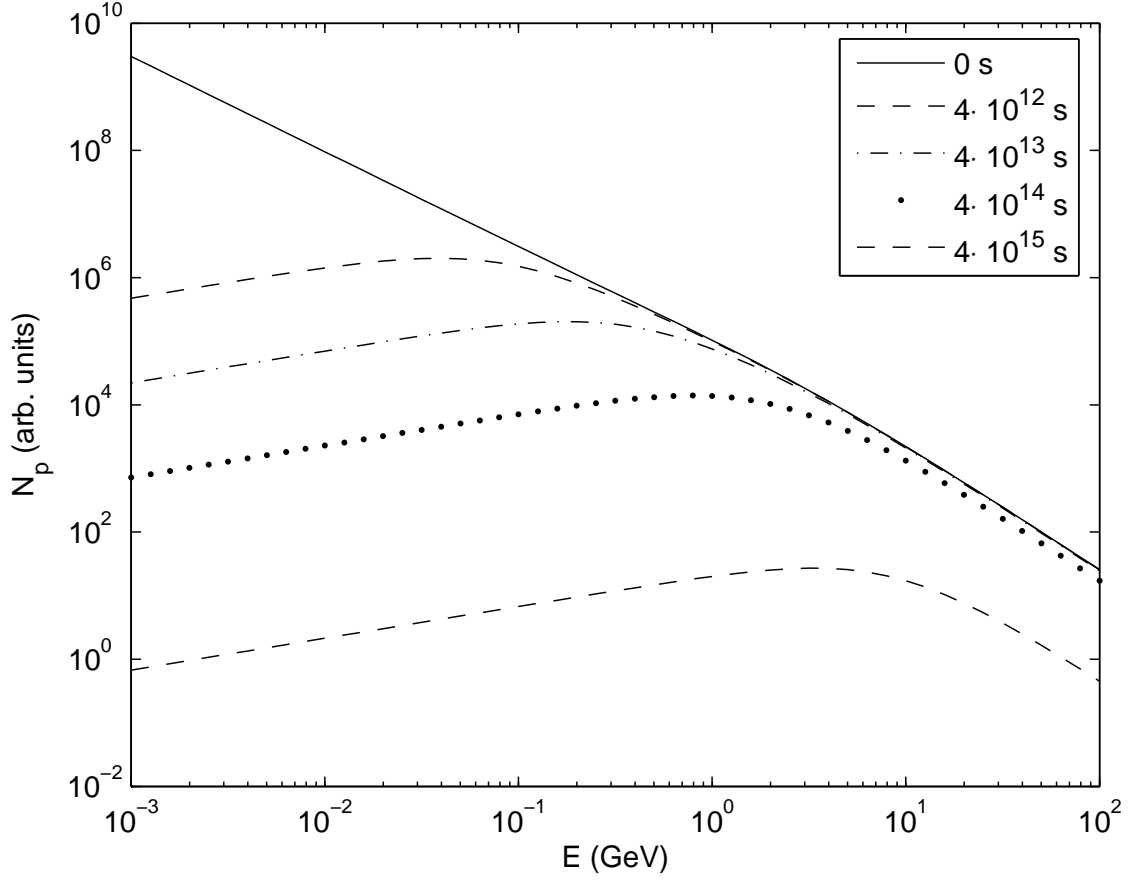


Fig. 2.— The spectrum of protons necessary at different moments of time for an ambient plasma density $n = 1 \text{ cm}^{-3}$.

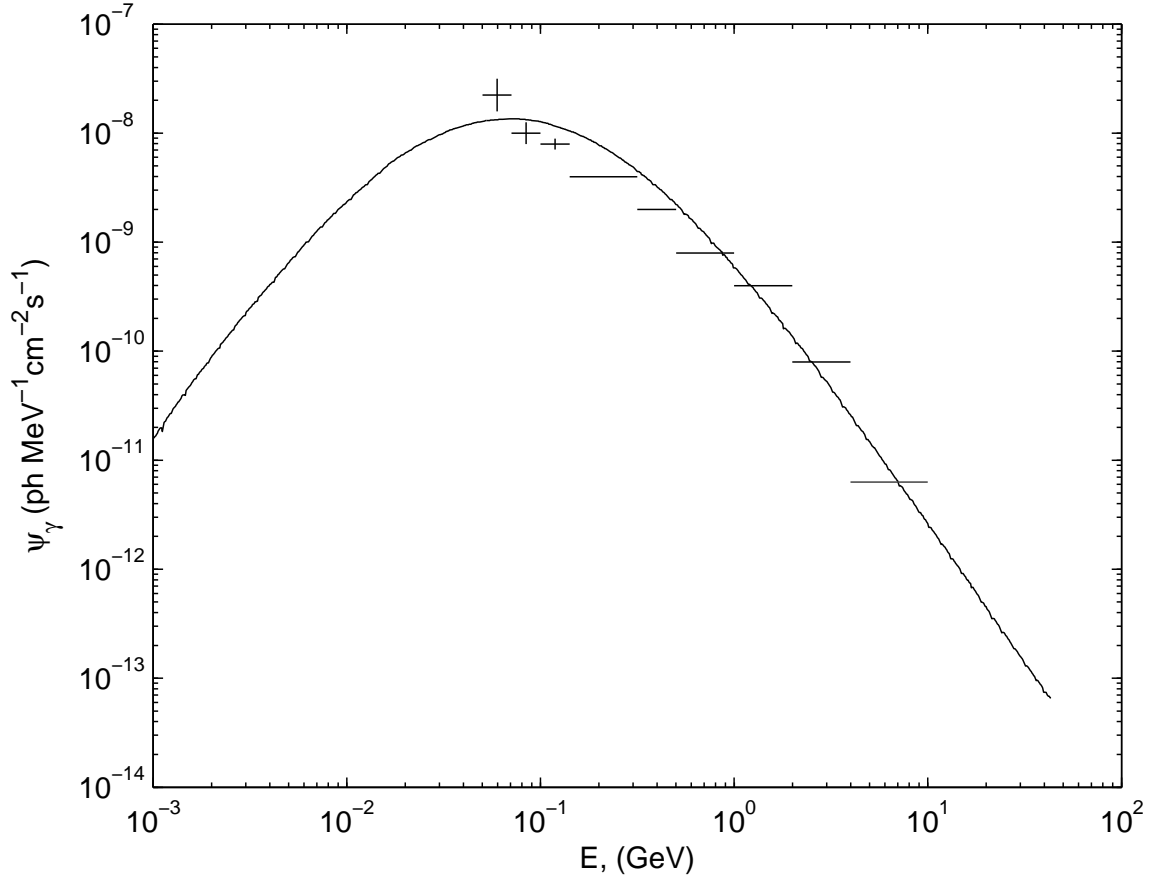


Fig. 3.— The flux of gamma-ray emission in the direction of the Galactic center measured with EGRET and the results of numerical calculations.

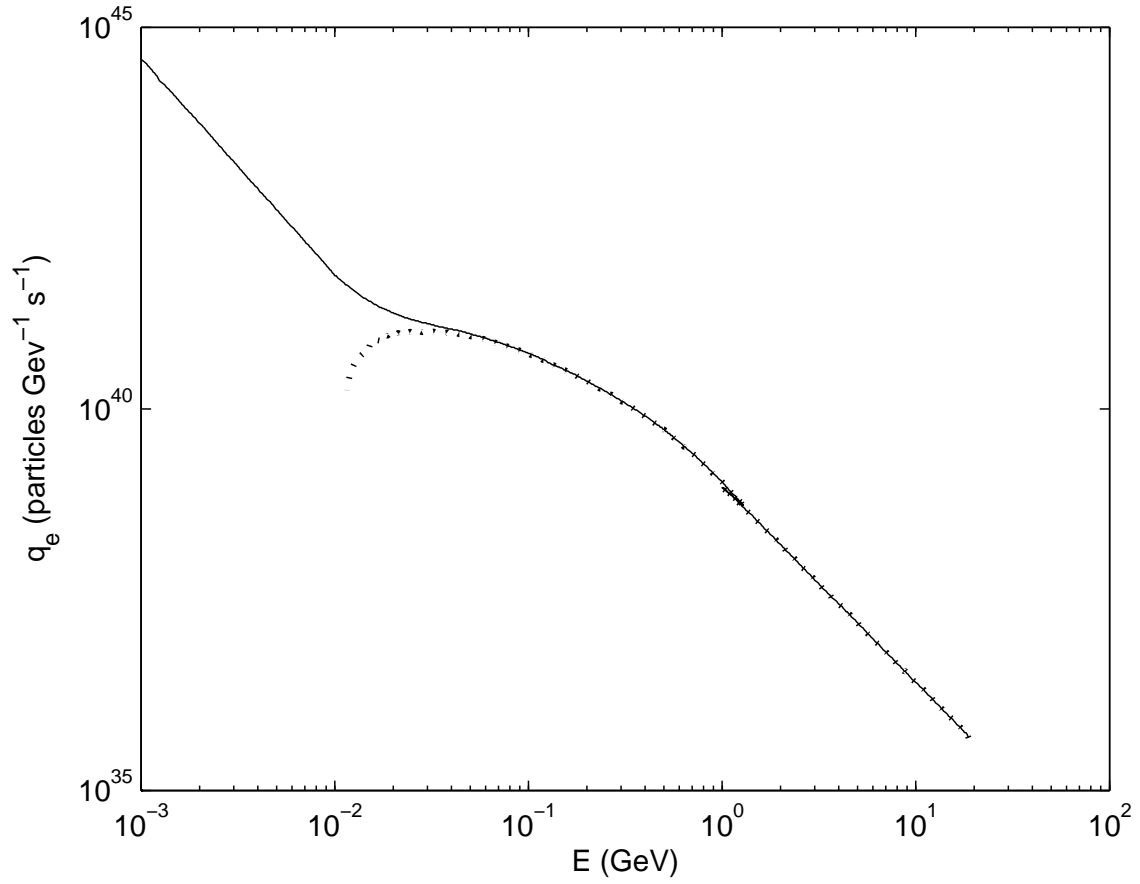


Fig. 4.— The total production function of secondary electrons from π^\pm -decay and Coulomb collisions (solid line) and the production function of positrons (dotted line).

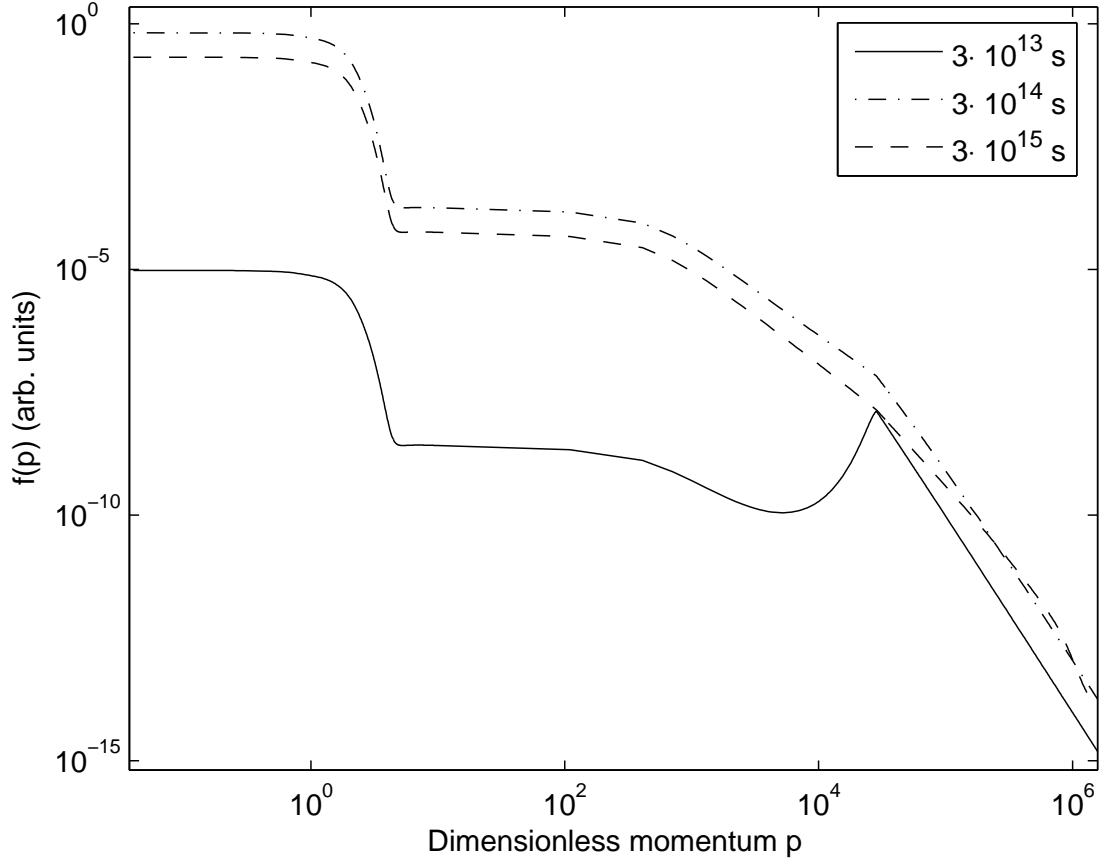


Fig. 5.— Time variation of the positron distribution function $f(p)$ for a gas temperature $T = 2.5$ eV. The dimensionless momentum is defined as $p/\sqrt{m_e kT}$ so the dimensionless momentum at unity corresponds to a positron with energy $\sim kT$.

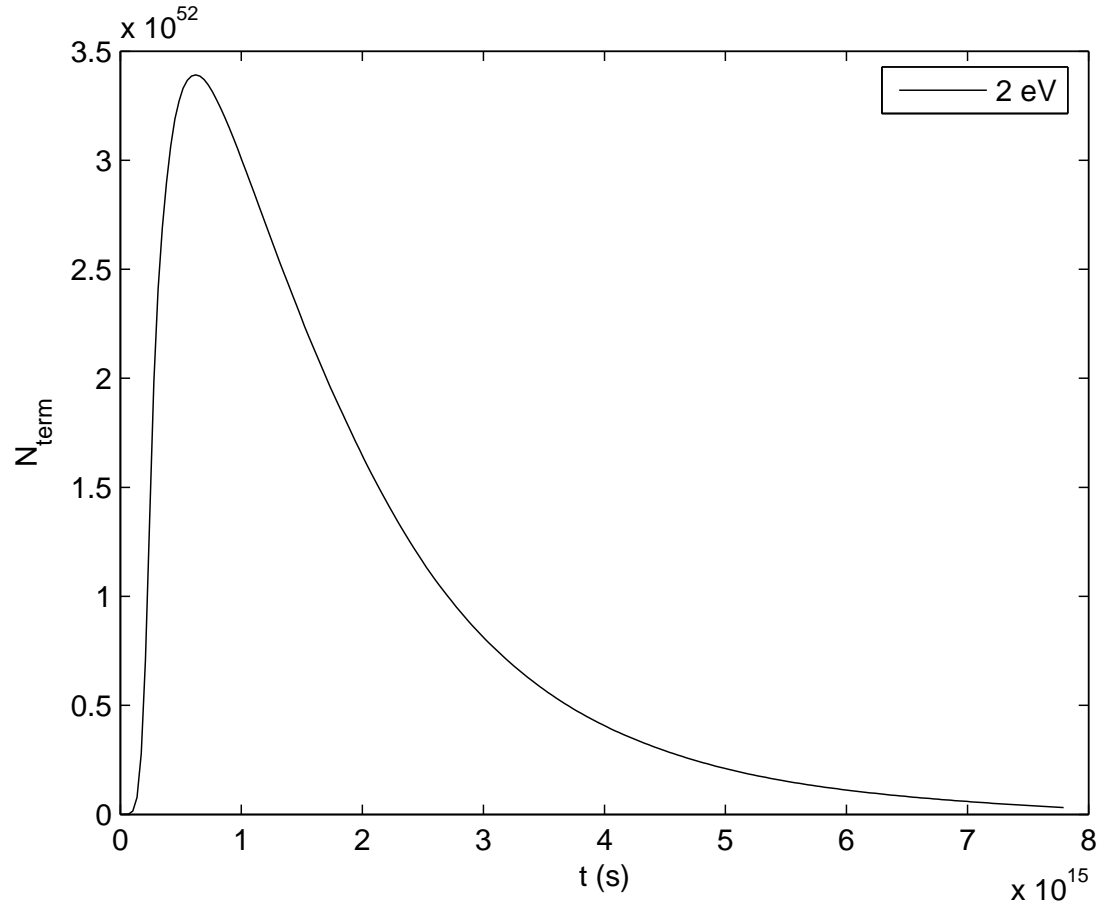


Fig. 6.— Time variation of the amount of thermal positrons produced by relativistic protons injected 4×10^{15} s ago in the gas with a temperature $T = 2.5$ eV and a density $n = 1 \text{ cm}^{-3}$.

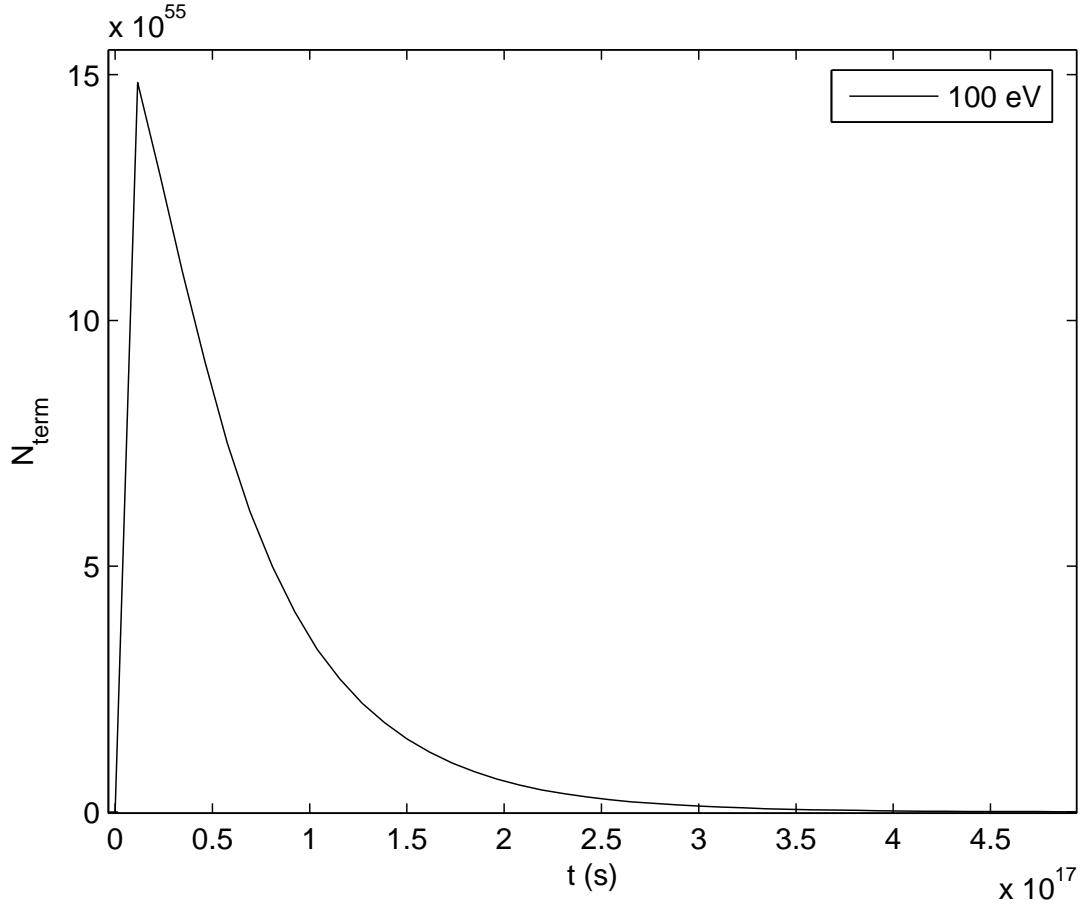


Fig. 7.— Time variation of the amount of thermal positrons produced by relativistic protons injected 4×10^{15} s ago in the gas with a temperature $T = 100$ eV and a density $n = 3 \times 10^{-3} \text{ cm}^{-3}$.

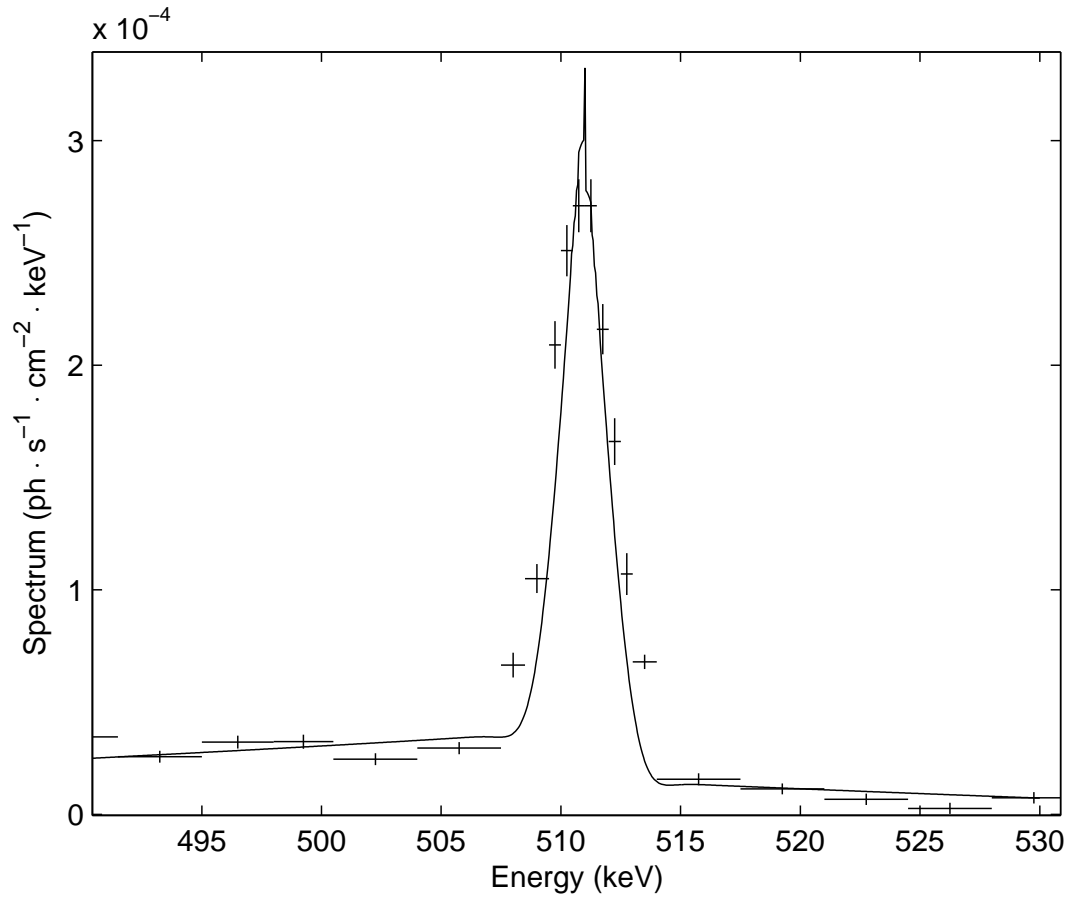


Fig. 8.— The total annihilation spectrum from a plasma with a temperatures 2.5 eV, together with the INTEGRAL data

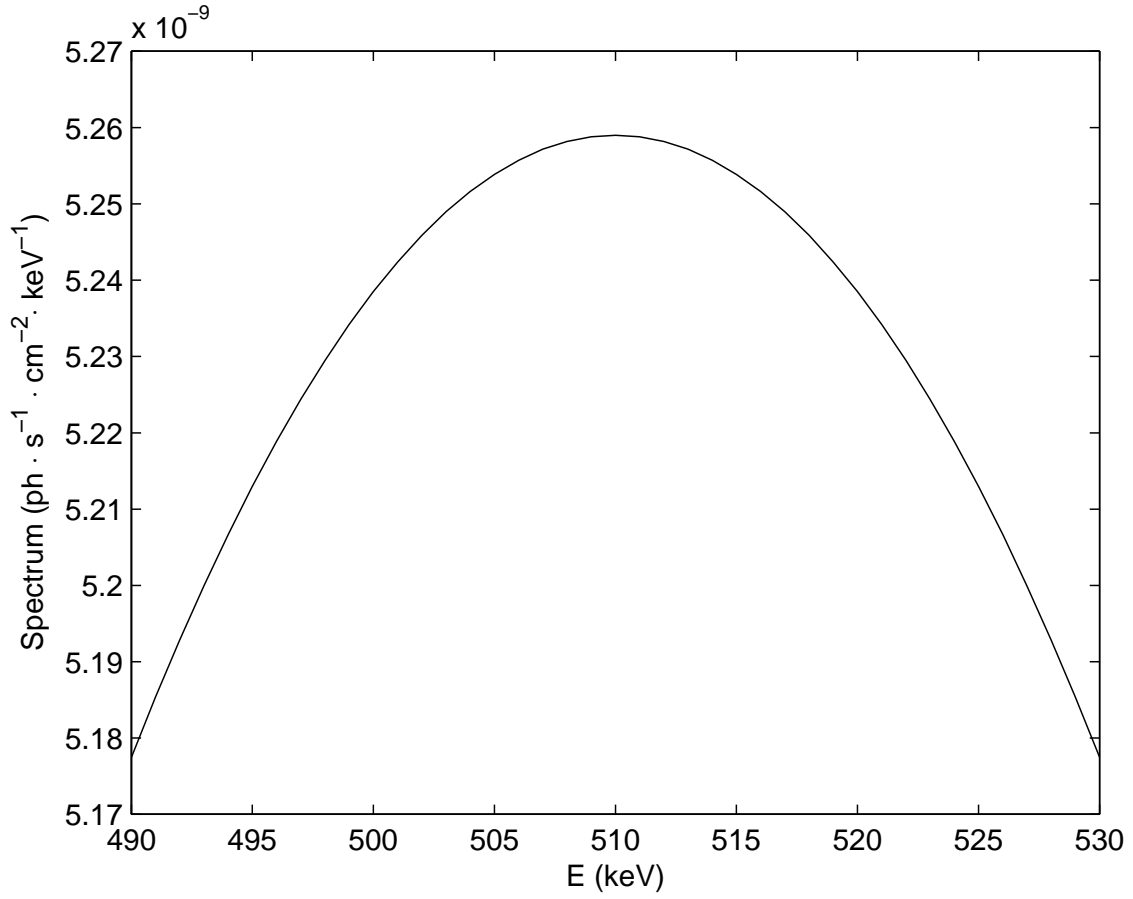


Fig. 9.— The annihilation flux from the hot plasma of the central region of radius ~ 0.7 kpc with a temperature of 100 eV, a density of $3 \times 10^{-3} \text{ cm}^{-3}$ and a filling factor of 30%.

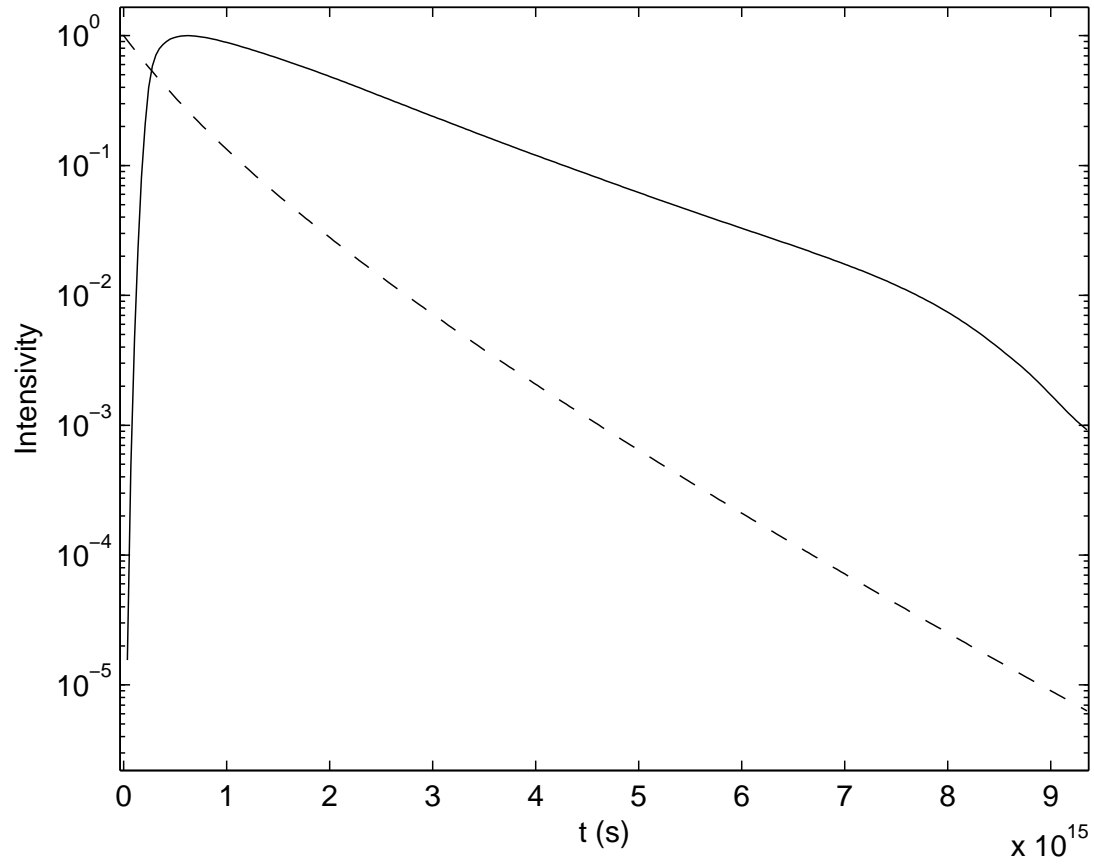


Fig. 10.— Time variation of the gamma-ray (dashed line) and annihilation (solid line) fluxes for a gas density $n = 1 \text{ cm}^{-3}$

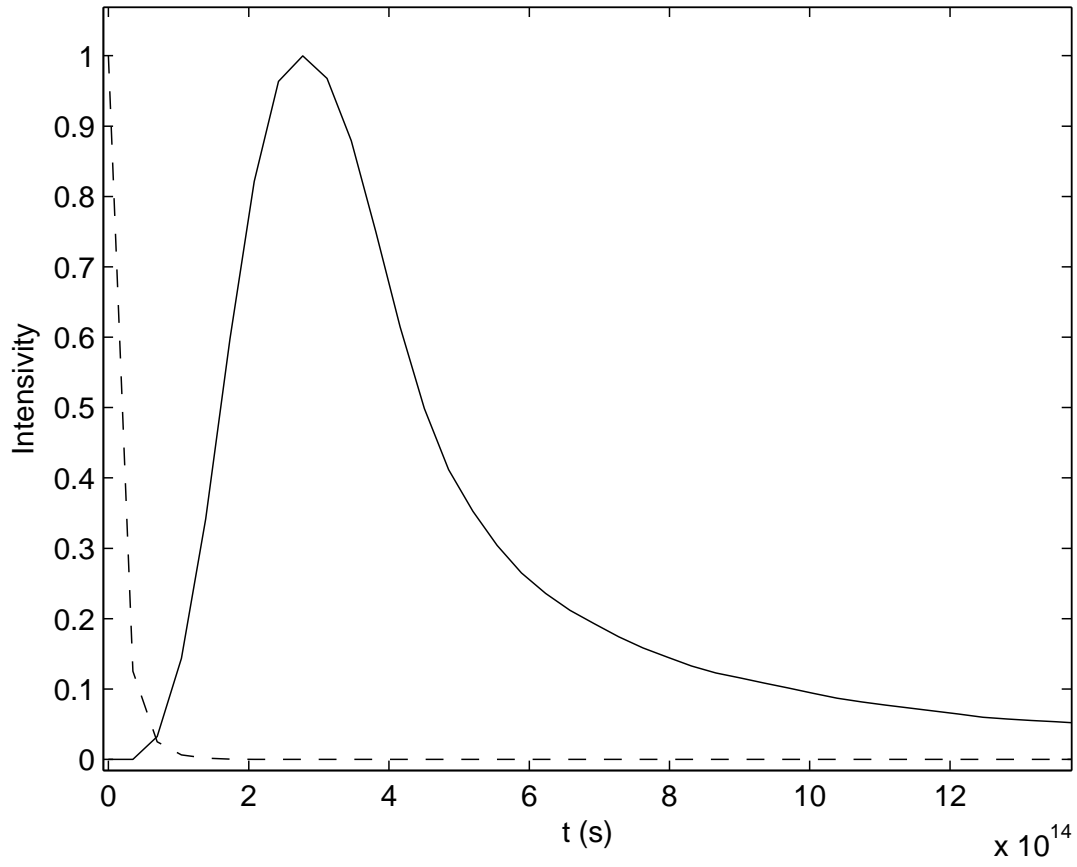


Fig. 11.— Time variation of the gamma-ray (dashed line) and annihilation (solid line) fluxes for a gas density $n = 30 \text{ cm}^{-3}$ for protons

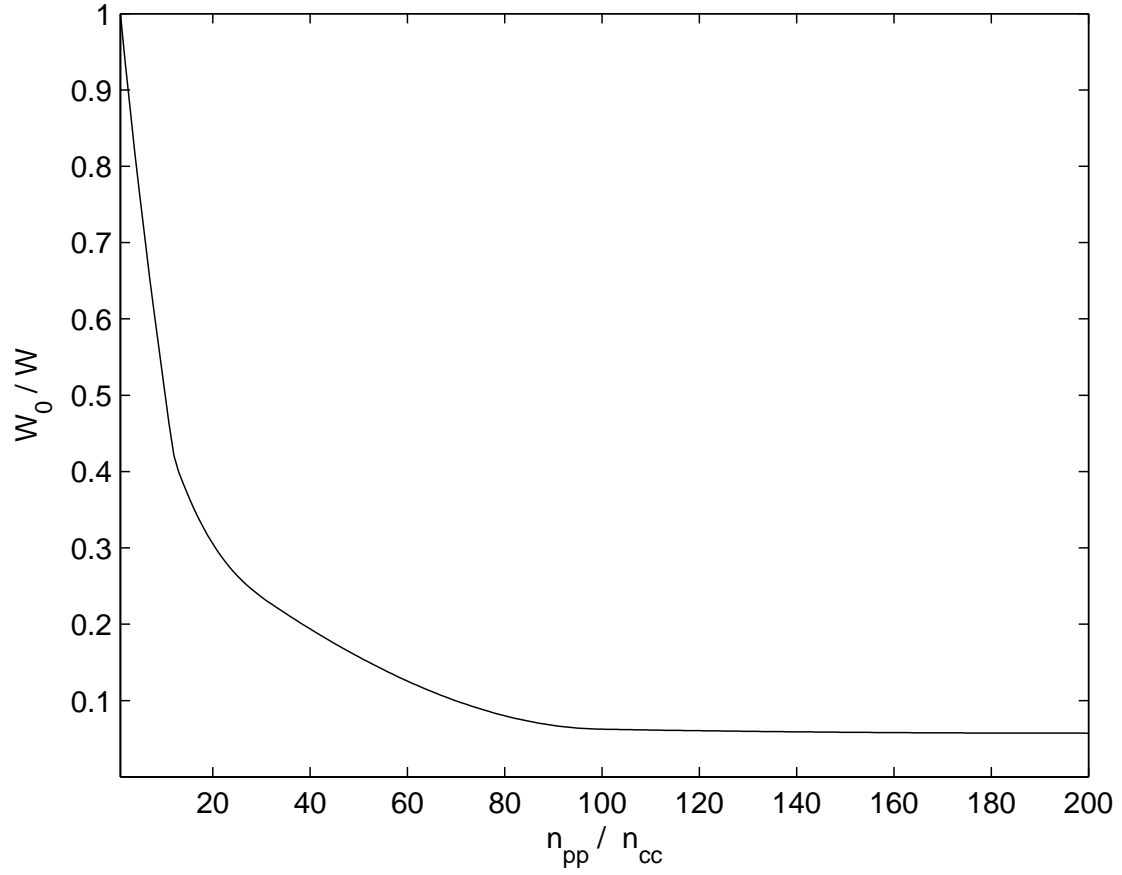


Fig. 12.— Variation of the proton energy output as a function of the ratio n_{pp}/n_{cc} . The output energy W_0 corresponds to $n_{pp}/n_{cc} = 1$

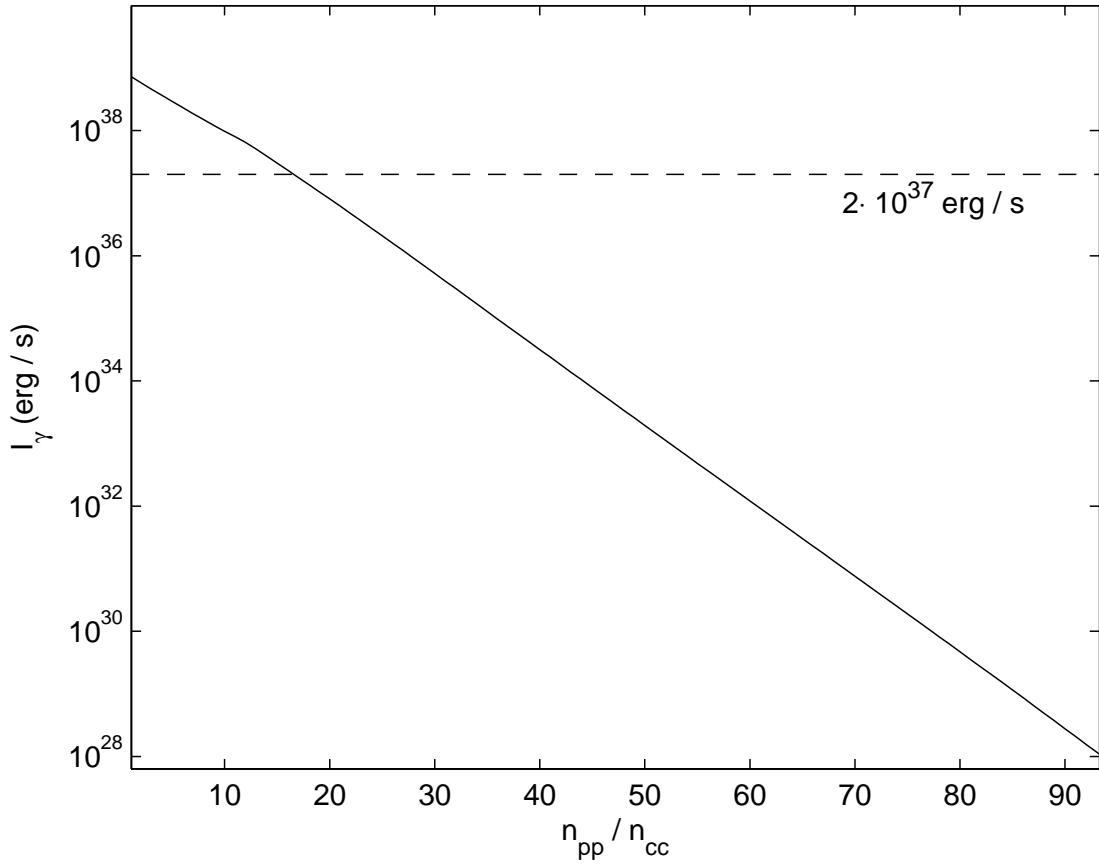


Fig. 13.— The expected gamma-ray flux at the moment when the production of thermal positrons reaches a value of $10^{43} \text{ e}^+ \text{s}^{-1}$ as a function of the ratio n_{pp}/n_{cc}

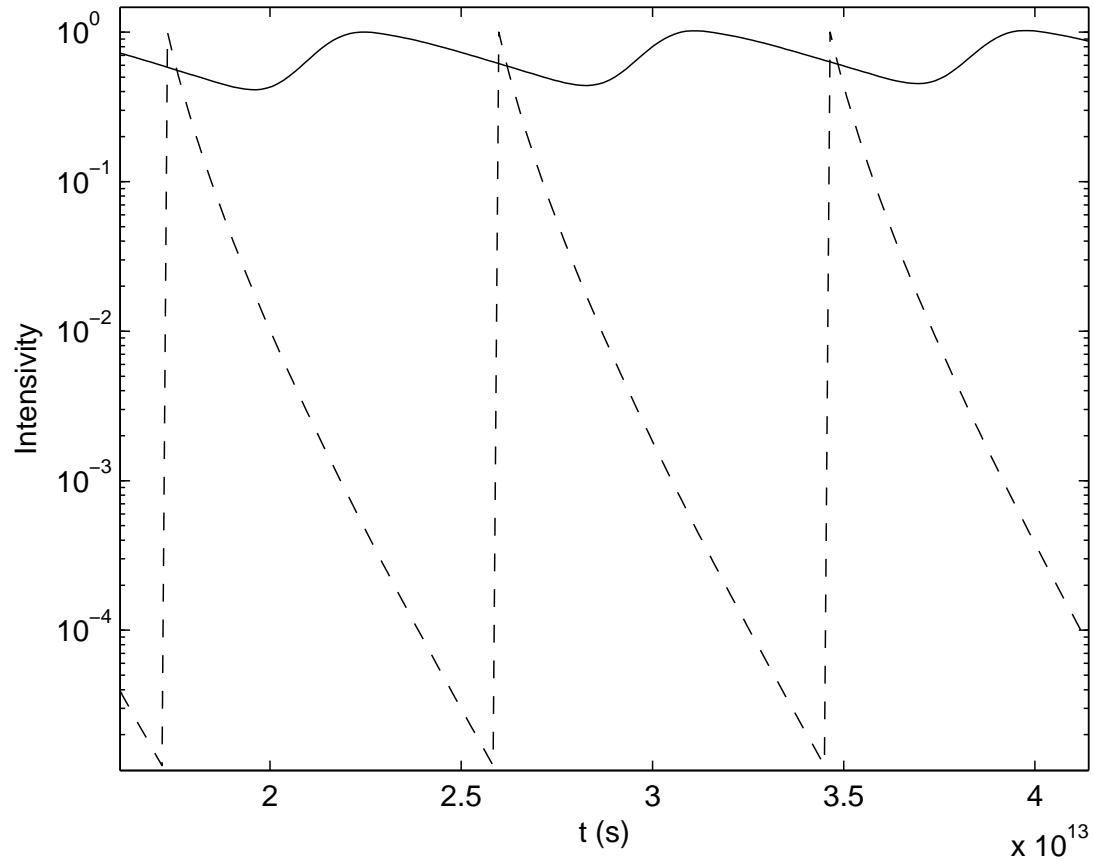


Fig. 14.— Gamma-ray and annihilation emission from several successive eruption of protons by the black hole. The parameters are presented in the text